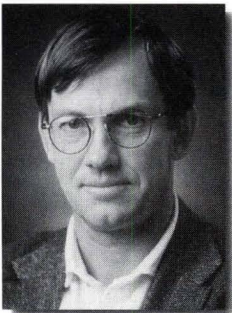
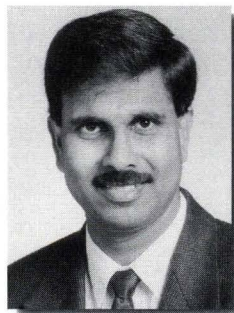


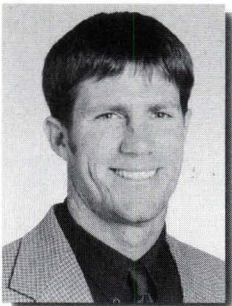
Preliminary Results and Conclusions From the PRESSS Five-Story Precast Concrete Test Building



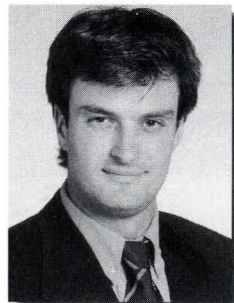
M. J. Nigel Priestley, Ph.D.
Professor of Structural Engineering
Department of Structural Engineering
University of California at San Diego
La Jolla, California



S. (Sri) Sritharan, Ph.D.
Assistant Project Scientist
Department of Structural Engineering
University of California at San Diego
La Jolla, California



James R. Conley
Graduate Research Assistant
Department of Structural Engineering
University of California at San Diego
La Jolla, California



Stefano Pampanin
Fulbright Visiting Scholar
Department of Structural Engineering
University of California at San Diego
La Jolla, California

A large-scale five-story precast concrete building constructed to 60 percent scale was tested under simulated seismic loading as the culmination of the 10-year PRESSS (Precast Seismic Structural Systems) research program. The building comprised four different ductile structural frame systems in one direction of response and a jointed structural wall system in the orthogonal direction. The test structure was subjected to seismic input levels equivalent to at least 50 percent higher than those required for UBC (Uniform Building Code) Seismic Zone 4. The behavior of the structure was extremely satisfactory, with only minimal damage in the shear wall direction, and no significant strength loss in the frame direction, despite being taken to drift levels up to 4.5 percent, more than 100 percent higher than the design drift level. The test validated the Displacement-Based Design (DBD) approach used to determine the required strength and confirmed the low damage and low residual drift expected of the building.

The Precast Seismic Structural Systems (PRESSSS) research program has been in progress for ten years, with the final phase of the program nearly complete. PRESSSS, sponsored by the National Science Foundation (NSF), Precast/Prestressed Concrete Institute (PCI) and Precast/Prestressed Concrete Manufacturers Association of California, Inc. (PCMAC), has coordinated the efforts of over a dozen different research teams across the United States to improve the seismic performance of precast/prestressed concrete buildings.

In the context of this paper, “buildings” refer to low- and high-rise buildings such as office buildings, parking structures, hotels, hospitals, multi-family housing, and other special structures. However, bridges and transportation structures are excluded.

Since the very beginning of the PRESSS program, all of the research teams involved in the program have focused their sights on two primary objectives:

- To develop comprehensive and rational design recommendations needed for a broader acceptance of precast concrete construction in different seismic zones.
- To develop new materials, concepts, and technologies for precast concrete construction in different seismic zones.

The first and second phases of the PRESSS research program have been completed. The third phase of the program comprises the design, erection and testing of a five-story precast concrete building using dry jointed construction. The purpose of this paper is to present the preliminary results and conclusions from this test.

As the key element of the final phase of the PRESSS research program, a 60 percent scale five-story precast concrete building was constructed and tested under simulated seismic loading at the University of California, San Diego (UCSD), California. The tests were carried out between June and September 1999.

The design of the building was based on concepts developed and tested in the earlier two phases of the PRESSS research program, which have been summarized by Priestley.¹ Details of the building design have also been described by Nakaki, Stanton and Sritharan,² and hence only a brief summary of the major design features of the structure is included here.

Fig. 1 shows a plan layout of the lower three floors of the building, which had a two-bay by two-bay configuration, with bay size 15 x 15 ft (4.57 x 4.57 m). Two different precast frames, one with prestressed beams, and the other using mild steel reinforcing bars across the beam-to-column connections provided lateral resistance

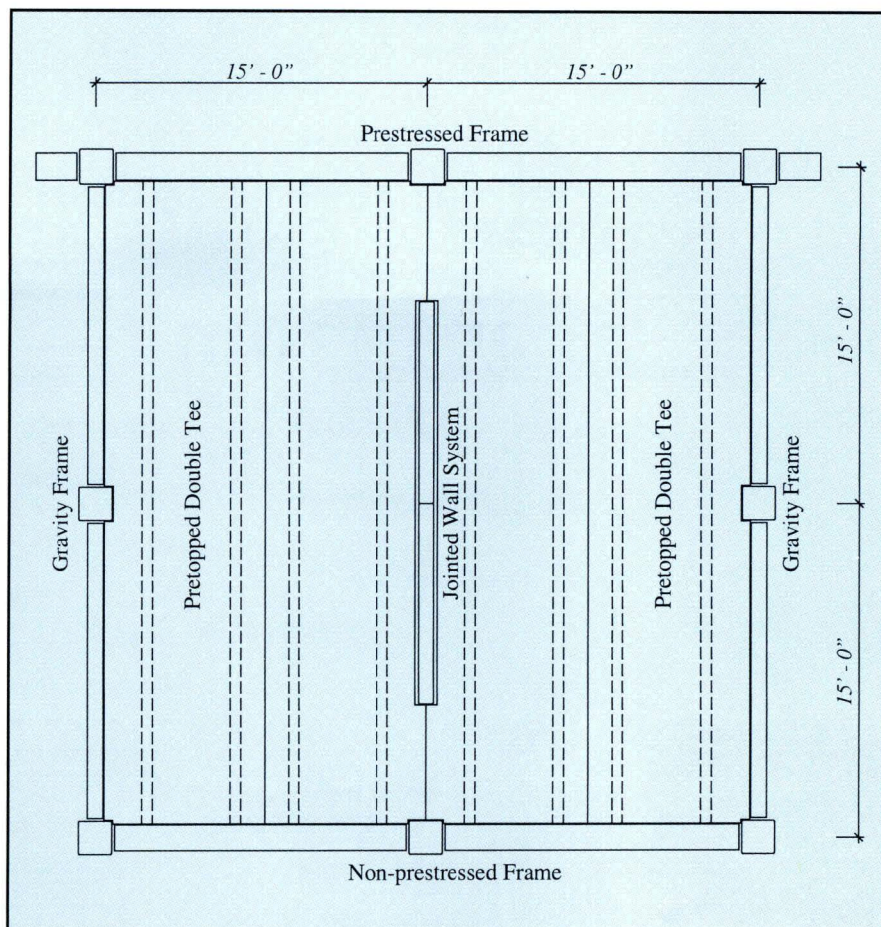


Fig. 1. Plan view of test building showing lower three floors.

at opposite sides of the building in one direction of response, with a central structural wall providing lateral resistance in the other direction. Non-seismic gravity frames without moment connection between beams and columns framed the test building boundaries parallel to the structural wall.

As shown in Fig. 1, the floor system for the lower three floors consisted of pretopped double tees spanning between the seismic frames, and connected to the center of each of the two wall panels comprising the structural wall. In the upper two floors, topped hollow-core slabs spanning between the gravity frames and the wall provided the floor system. The hollow-core slabs were connected to each other and the seismic frames with a cast-in-place topping.

Although the plan dimensions of the test building were comparatively modest, it should be recognized that the tributary floor area in the prototype building, on which the test building was based, was substantially larger

than what is shown in Fig.1. Vertical support to the extra area was provided by additional gravity frames which did not contribute to the seismic resistance of the building.

In order to obtain the maximum possible information from the test building, five different structural systems were investigated in the same structure. The four different ductile frame systems tested are illustrated in Fig. 2.

The lower three floors of the prestressed concrete frame consisted of hybrid connections (see Fig. 2a) with single-bay beams connected between continuous columns by unbonded post-tensioning. Additional flexural strength and damping was provided by mild steel reinforcing bars slid through corrugated ducts in the beams and columns, and grouted solid with short unbonded lengths in the beams to reduce peak strains under seismic response.

In the upper two floors of the prestressed concrete frame, continuous precast rectangular beams with preten-

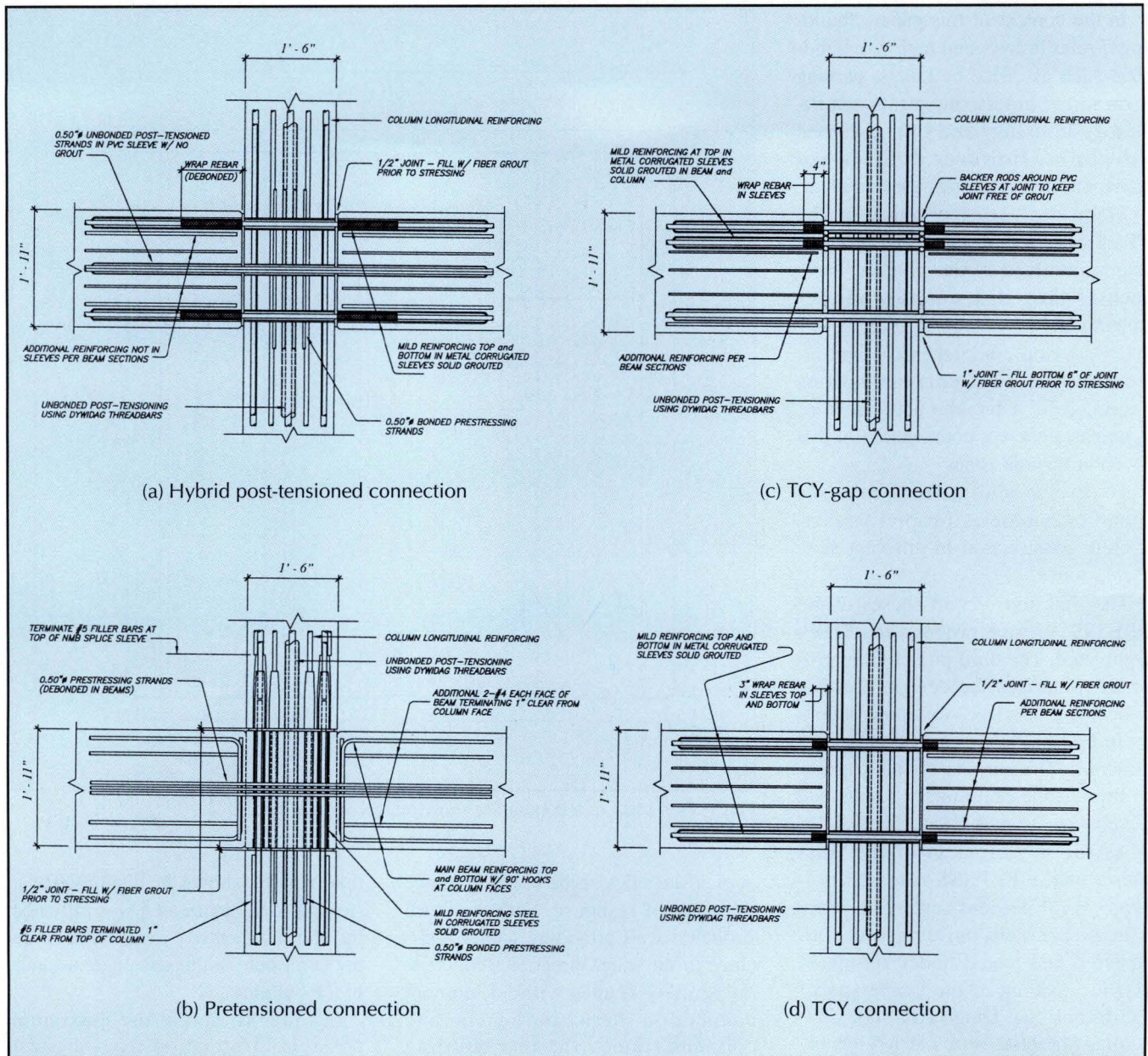


Fig. 2. Seismic frame connection types.

sioned strands bonded in external stub beams, but debonded over the interior beam length between the column faces provided seismic resistance (see Fig. 2b). No additional mild steel reinforcement was provided across the beam-column interfaces. The full length pretensioned beams were threaded over column reinforcing bars extending from the top of the columns, with reinforcing bar splices providing column continuity.

Moment resistance over the lower three floors of the non-prestressed frame was provided by TCY-gap connections (TCY denotes tension/compression yielding), as illustrated in Fig. 2c. At the bottom of the connec-

tions, the beams were clamped to the column by unbonded post-tensioning threaded bars reacting through fiber grout pads over the bottom part of the connection only. Over the top two-thirds of the connection, a 1 in. (25 mm) gap was provided.

Mild steel reinforcement slid through corrugated ducts and grouted solid in the beams and column was designed to yield alternately in tension and compression, for negative and positive moments, respectively, without unloading the precompression across the bottom grout pad. As a consequence, all rotation at the beam-column interface would occur by opening or closing of the gap at the top of the

connection. Over the top two floors of this frame, moment capacity was provided by the TCY connection using mild steel reinforcing bars in grout ducts at the top and bottom of the connection, thus approximating the behavior of a conventional reinforced concrete connection with equal top and bottom steel (see Fig. 2d).

In the orthogonal direction, the structural wall consisted of four precast panels, each two and a half stories tall (see Fig. 3). The panels were vertically connected to each other and to the foundation by unbonded vertical post-tensioning, using threaded bars. A horizontal connection across the vertical joint was provided by stain-

less-steel energy-dissipating U-shaped flexure plates, welded to embed plates in both adjacent wall panels. In addition to providing energy dissipation, these plates provided additional lateral resistance by shear-coupling between the two structural walls.

The structural design was carried out in accordance with Direct Displacement-Based Design (DBD) principles which have been described by Priestley et al.^{1,3,4} The chosen design criterion was such that the structure should achieve a maximum lateral drift of 2 percent under seismic excitation equivalent to UBC (Uniform Building Code) Zone 4, for an intermediate S_c soil. More complete details of the design procedure and the design details are available in a recent paper by Nakaki et al.²

Erection of the building was carried out inside the Charles Lee Powell Structural Laboratory of UCSD, one of the largest structural testing facilities in the United States. Despite the restricted space and special constraints, erection of the test building was completed within 12 working days. Because of page limitations, construction details regarding the assembly of the test building will not be described here, but will be the subject of a separate paper, to be published later as part of a series of final papers on the project.

TEST SEQUENCE

Lateral forces and displacements were applied to the building by two actuators at each floor level, each connected to the floor by actuator extensions and a triangulated connection detail, shown in Fig. 4. With this detail, the actuator load was equally distributed to the two bays, and relative horizontal displacement between the two connection points on the floor was possible.

One consequence of the connection detail was that since the actuator was located above the floor level, the connection detail imposed vertical forces on the floors, in addition to the horizontal forces. Equal displacements were applied to the two actuators at each floor level at all stages of the test.

The objective of the experiment was to test the structure under a series of

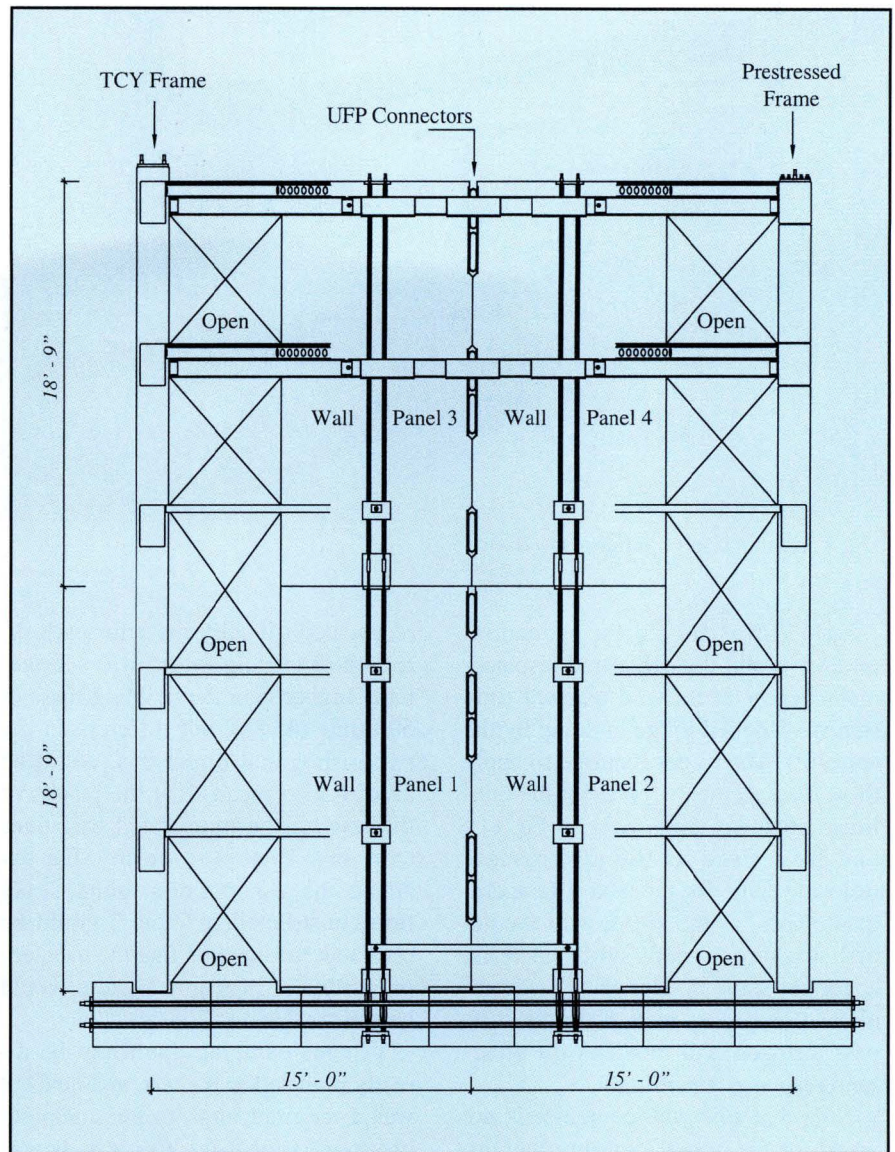


Fig. 3. Jointed structural wall elevation.

earthquake levels. These seismic levels were chosen to conform to different limit states recommended by the Structural Engineers Association of California (SEAOC).⁶ As shown in Fig. 5a, four different earthquake levels are defined, corresponding to 33, 50, 100 and 150 percent of the design level earthquake.

The principal method of testing the building was pseudodynamic testing, using spectrum-compatible earthquake segments, scaled in frequency and amplitude from recorded accelerograms to match the design spectrum at 5 percent damping. An example of the agreement between the design spectrum and the accelerogram segment for the design level event (EQ3 in Fig. 5a) is shown in Fig. 5b. More details on the test program are available in Refs. 7, 8 and 9.

The concept of pseudodynamic testing is described in Fig. 6. The computer controlling the displacement input to the actuators contained a simple five-degrees-of-freedom model of the building, initially calibrated by low-level flexibility tests, as described subsequently. This model was subjected to inelastic time-history analysis under the specified earthquake record.

The structural response is governed by d'Alembert's equation of motion:

$$[M]\ddot{x} + [C]\dot{x} + [K]x = -[M]a_g \quad (1)$$

where $[M]$, $[C]$, and $[K]$ are the mass, damping and stiffness matrices, and \ddot{x} , \dot{x} and x are the relative acceleration, velocity and displacement vectors, and a_g is ground acceleration.

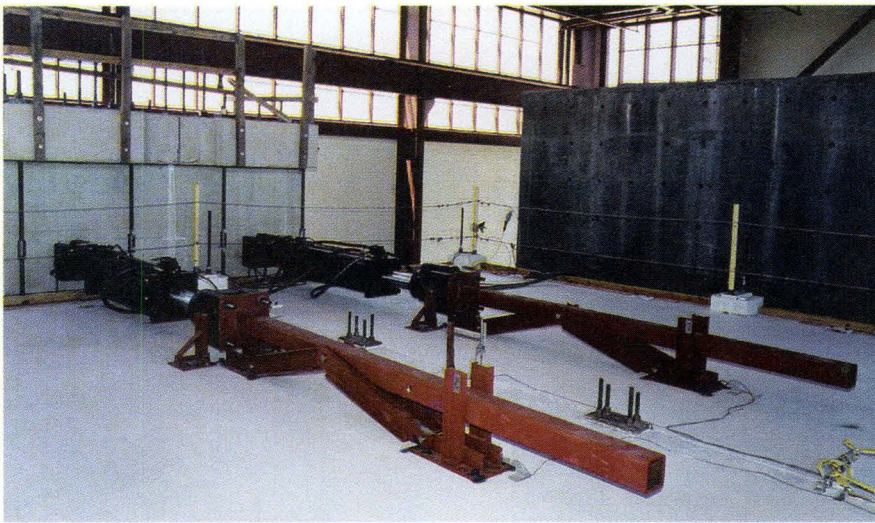


Fig. 4. Connection of actuators to floor.

Eq. (1) was solved for sequential time steps and the calculated displacement vector at the end of each time step was applied to the building by the actuators. The forces required to apply these displacements represent the nonlinear stiffness terms $[K]x$ in Eq. (1), and were used as the appropriate restoring force for the next time increment. Thus, as the stiffness of the actual structure is modified by inelastic action, or strength degradation, the analytical procedure recognizes the stiffness changes, and modifies the structural response accordingly.

Note that since the computer is not aware of the actual building weight, the mass vector is a required input to the program. This meant that the cor-

rect scaled tributary mass for each direction of loading, which was substantially higher than the building mass of 500 tons (454 t), but different in the two orthogonal directions, could be used. It also means that the results of the test can be interpreted for zones other than Zone 4 seismicity. For example, the response of a similar structure constructed in Zone 2 could be obtained, recognizing that the tributary mass for the structural system would be greater than for Zone 4.

Viscous damping could not be directly modeled in the test, and hence it was a required input to the computer program controlling the test. It was necessary, for design and testing equivalence, for the same assumptions

about elastic viscous damping to be made for the design models, and the physical test. Since the design was based only on the first inelastic mode of response, this equivalence was only required for the first mode. As discussed subsequently, it was necessary to apply higher damping values to higher modes at later stages of the testing.

Since the initial input to the building was based on an initial estimate of elastic stiffness, flexibility tests were periodically carried out at different stages of the test sequence. In these tests, actuator forces were applied sequentially and independently to the five floor levels, with displacements at each of the floors being recorded for each floor force input. This enabled the flexibility matrix to be established, and after inverting and smoothing, the initial stiffness matrix was defined.

The initial stiffness matrix was also needed in the iteration procedure used to obtain the required displacements at each time step. Displacements defining the structural response were directly measured on the structure, whereas the command displacements were applied and monitored by internal transducers in the actuators. Inevitably, a discrepancy between command and external response displacements existed, primarily due to flexibility in the load path.

To remedy this situation, an error correction procedure was carried out,

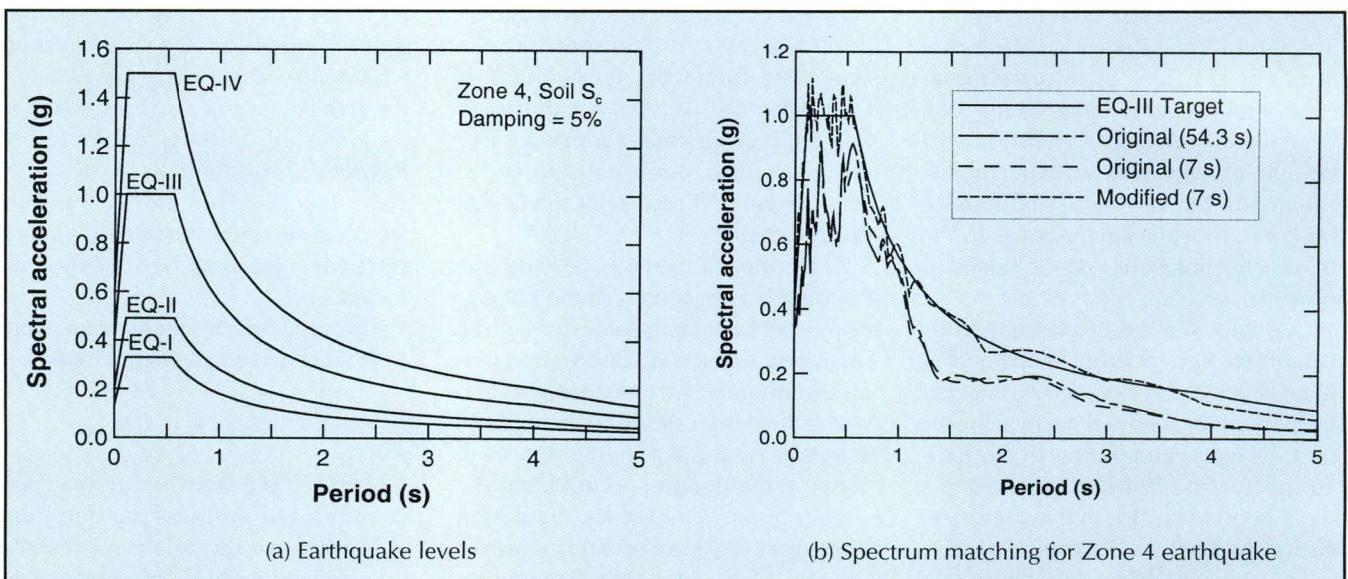


Fig. 5. Earthquake excitation and spectrum matching.

multiplying the vector of displacement errors by the initial stiffness matrix, and applying the resulting floor forces as corrections. This procedure was iteratively carried out until the displacement errors at each floor level were within a predetermined tolerance. Further details on multi-degree-of-freedom pseudodynamic testing are found in Ref. 10.

The third type of test carried out involved cyclic testing under a force vector in the form of an inverted triangle to specified roof-level displacements. After each earthquake input, one or two complete cycles of response were applied to the peak displacement achieved during the pseudodynamic sequence. This was done for three reasons:

First, the pseudodynamic sequences did not exercise the structure to the same displacements in each direction (positive and negative). The inverted triangle test exercised the building to the same peak displacement in both directions.

Second, the pseudodynamic sequences, though matching the required spectrum were comparatively short, as a consequence of the time taken to actually apply the record (typically, 20 to 30 minutes per second of earthquake record). As a consequence, only one displacement peak to maximum response was typically achieved in the tests. The inverted triangle tests enabled the structure to be subjected to more cycles at peak response.

Third, during the inverted triangle tests, the test was halted at each displacement peak, to enable the physical condition of the building to be examined, cracks marked, and photographs taken.

Initial testing was carried out at a fraction of the EQ1 level (see Fig. 5a) to enable the test control to be refined. Following this, the seismic intensity was gradually increased up to the maximum level. Table 1 lists the tests carried out in each direction of response.

The wall direction was tested first, with actuators reacting against a specially constructed precast reaction wall. During application of the maximum earthquake segment of $1.5 \times EQ3$ (equivalent to EQIV in Fig. 5a), the displacements of the precast reaction

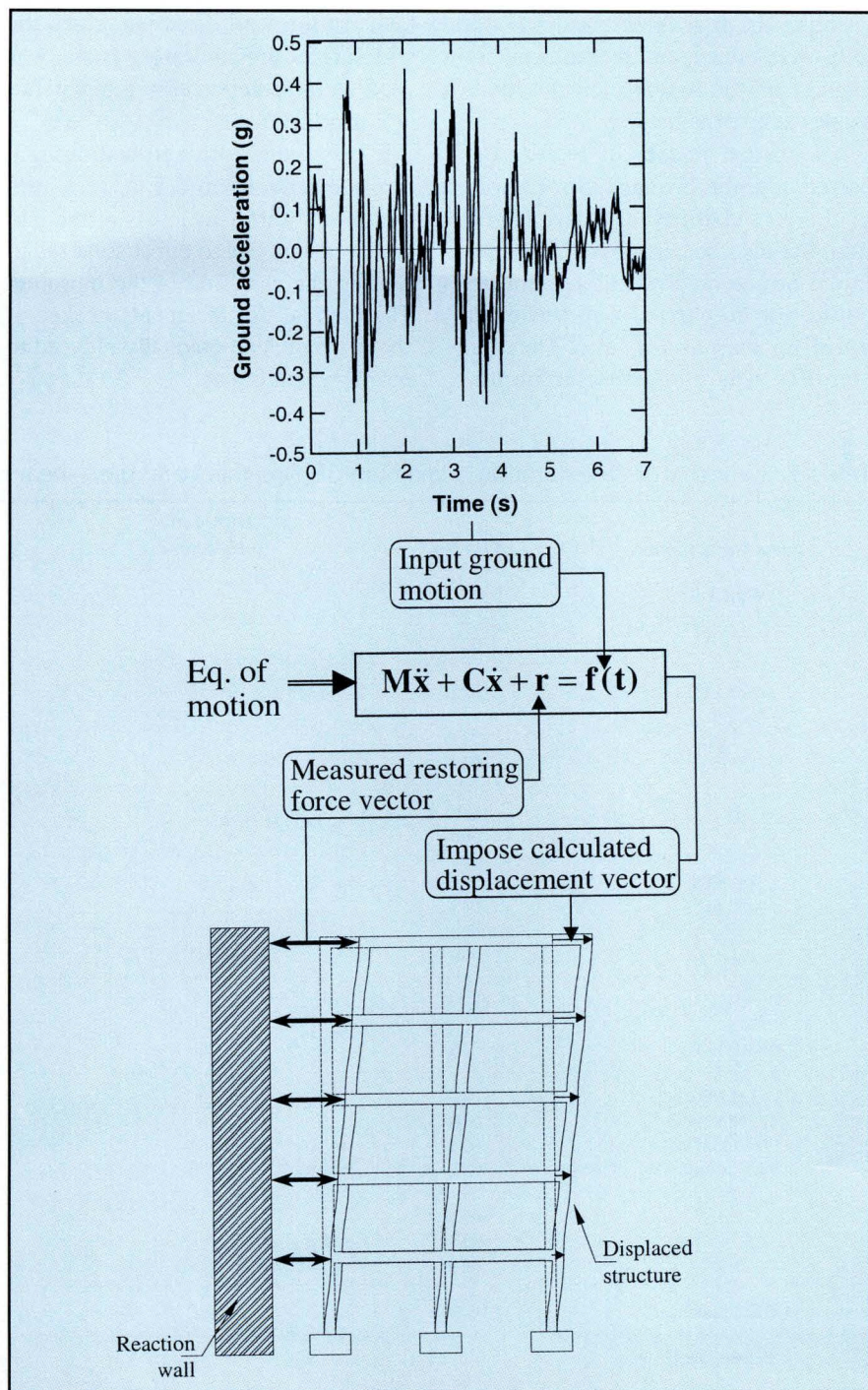


Fig. 6. Concept of pseudodynamic testing.

wall exceeded the safe maximum value, and as a consequence the subsequent inverted triangle force input was not applied in this direction. Actuators were then moved to the frame direction and testing was continued.

In the frame direction, it was found that higher mode story force levels at EQ3, the design level of input were significantly higher than anticipated, and the connections of actuator to floor, and floor to frame were exceeding design ultimate values. As a con-

sequence, subsequent testing was only carried out using the inverted triangle force pattern, which exercised the structure to maximum displacements, but did not input the higher mode story force levels. This is discussed further in the results section of this paper.

Dynamic characterization of the building was carried out using a shaker attached to the top of the building before the start of the frame test program, and also after its completion,

enabling the first three elastic modes to be determined, and the influence of damage on the frequencies and mode shapes to be examined.

All critical phases of testing occurred at night, primarily for reasons of thermal stability of instrumentation, but also because other activities in the Structural Systems Laboratory could not be carried out while the building was under test. Thermal stability was of particular impor-

tance in the wall direction, since the structure of the laboratory frame was used as the reference system for lateral displacements.

It was found, prior to testing, that displacements up to 0.1 in. (2.5 mm) occurred at different levels of the laboratory frame due to direct solar radiation on the east side in the morning. The thermal displacements peaked at about 1 p.m., and gradually reduced to zero by about 8 p.m.

INSTRUMENTATION AND DATA RECORDING

Primary data recorded included the actuator forces and displacements, and the displacements at each side of the building at each floor level. These latter displacements were recorded at the transverse centerline of the building for the test direction considered.

Wall uplift displacements at the base, and relative vertical displace-

Table 1. Summary of time duration, maximum displacement and base shear for wall and frame tests.

Beam Designation	Test No.	Duration (pseudo-time)	Δ -Max (in.)**	Base Shear (kips)**
Wall Test				
IT 0	023		0.15	71.4
0.25 EQ1	025	2.952	0.20	80.5
0.5 EQ1	032	3.972	0.41	142.3
1.0 EQ1	033	3.972	1.22	315.3
IT 1	034*		1.25	186.6
	036		1.25	174.3
1.0 EQ1	038	3.0	1.70	286.4
-1.0 EQ1	039	3.972	1.78	292.6
1.0 EQ2	040	5.304	3.00	294.7
IT 2	041*		3.00	221.3
-1.0 EQ2	046	5.208	2.84	299.4
1.0 EQ3	047	0.6	2.10	302.5
1.0 EQ3mod	049	0.6	2.07	214.5
1.0 EQ3mod2	050	0.606	1.94	260.9
1.0 EQ3mod5-10	051	5.772	8.31	321.5
IT 3	052		8.31	278.2
	053		2.00	217.9
	054		8.31	278.2
-1.5 EQ3mod5-10	055*	5.688	11.6	464.9
Frame Test				
0.25 EQ1	107	3.972	0.57	120.7
0.5 EQ1	108*	3.972	1.17	201.2
1.0 EQ1	110	3.972	2.63	340.8
IT 1	111		2.63	258.1
1.0 EQ2mod	112	5.304	6.84	333.2
IT 2	113*		6.86	342.8
1.0 EQ3mod5-10	116	3.408	9.85	353.5
IT 3	117		10.00	349.3
IT 4	119		11.88	347.1
IT 5	120		18.58	369.9

* Flexibility test performed.

** Absolute value.

Note: 1 in. = 25.4 mm, 1 kip = 4.45 kN.

ments across the central joint were also recorded at the base and top of the wall. Potentiometers were placed to measure overall beam elongations, and also, in the form of transducer arrays on selected joints, to monitor joint deformations. In addition, a large number of electrical resistance strain gauges were placed on reinforcing bars in a number of locations.

At the time of writing this preliminary report, many of these data remain unexamined, and will be reported on at a later stage. In this paper, overall structural performance, recorded in the form of forces and displacements, will be of prime interest.

In addition to electronic instrumentation, the condition of the building was recorded by photographers, after marking cracks with felt pens. To facilitate crack detection, the entire building was painted with a white undercoat prior to testing. Time-lapse video recording, using three cameras, was made at all the critical loading stages. Fig. 7 shows a general view of the building during the test.

TEST RESULTS

Discussed herein are the general observations and force-displacement characteristics in the wall direction and frame direction of loading.

Wall Direction of Response

General Observations — In the wall direction of loading, the design drift under the design level earthquake (Zone 4 intensity) represented a roof level displacement of 9 in. (228 mm). Under EQ3, the peak recorded displacement was 8.3 in. (211 mm), 8 percent below the target design displacement. This is considered to be a very satisfactory result, and a good verification of the displacement-based procedure used to design the structure.

Damage to the building when tested in the wall direction was minimal, even after subjecting the structure to an earthquake of intensity 50 percent higher than the Zone 4 level input motion. No cracking developed in the wall, except at the base connection to the foundation. Fig. 8a shows the condition of the walls at the location of the lower U-shaped flexure plates connecting the walls.

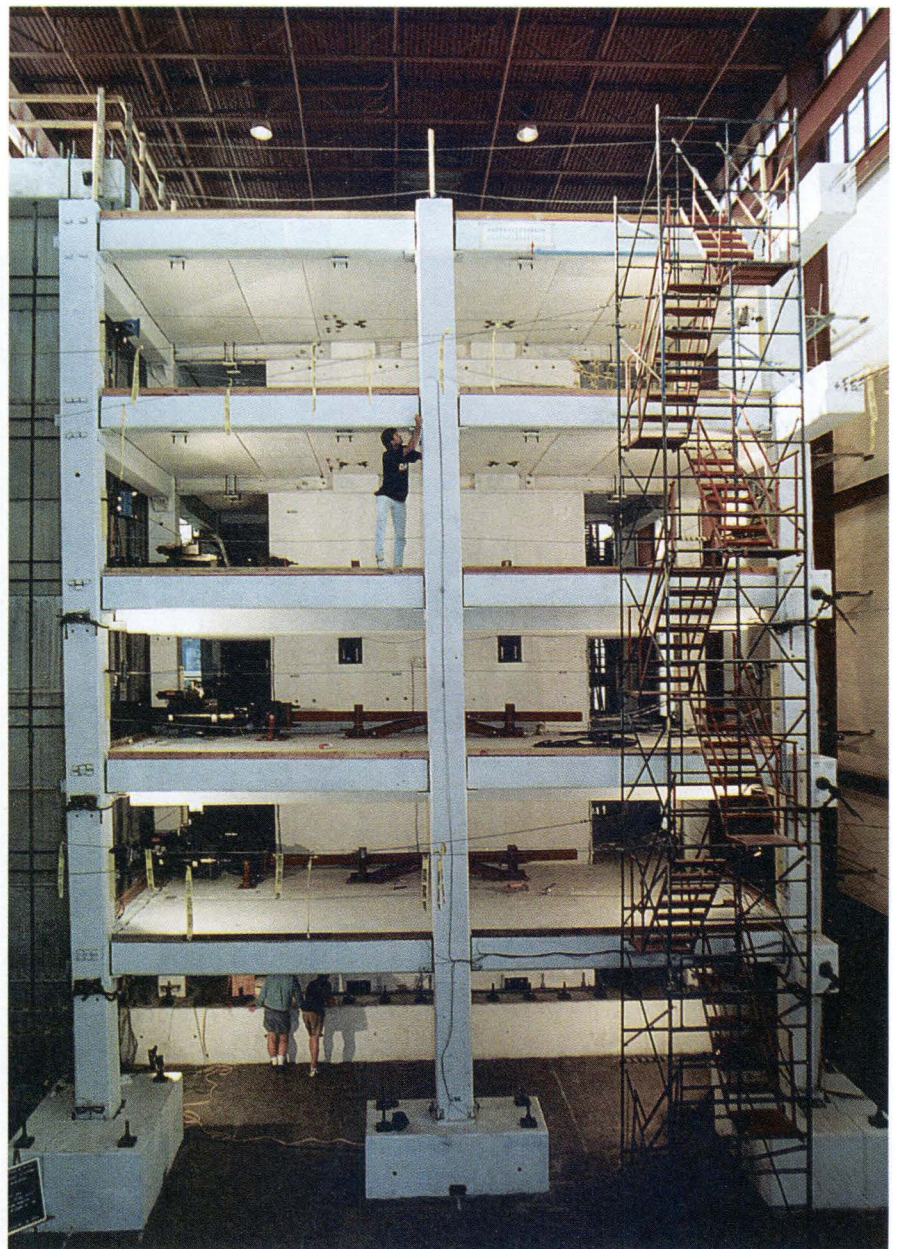


Fig. 7. Overall view of five-story building under test.

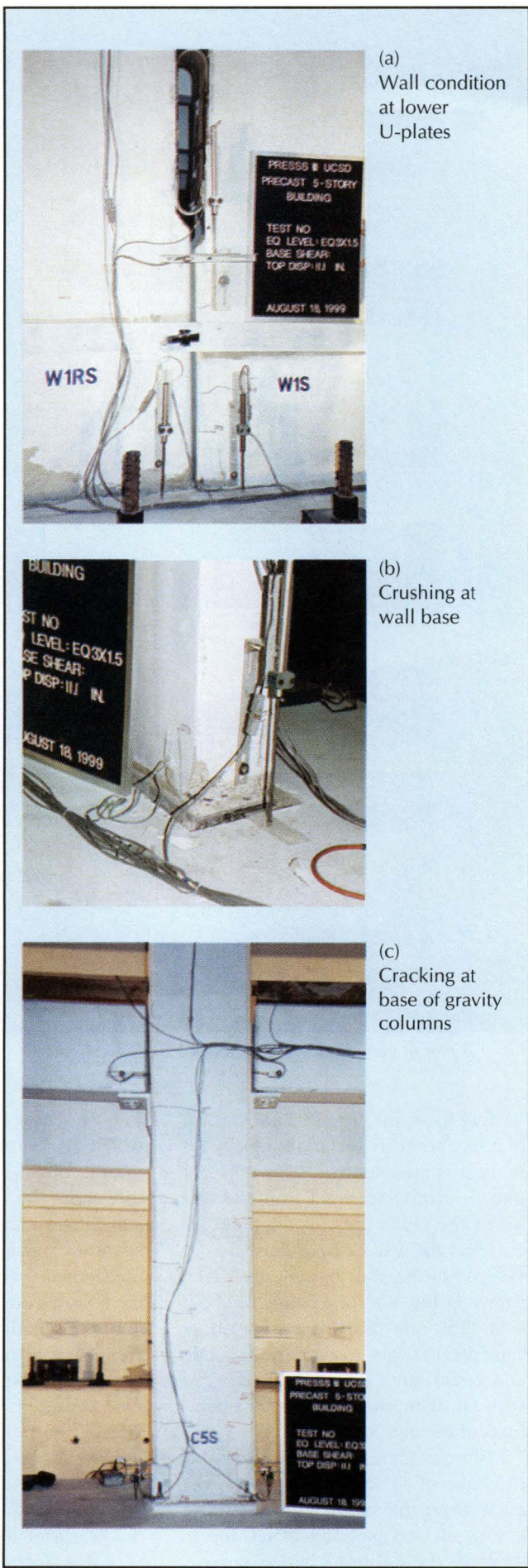
necting the walls. The relative vertical displacement at the maximum roof level displacement of 11.6 in. (294 mm) is clearly apparent from the offset of the lower ends of the plate recesses in the walls. Minor crushing developed at the wall base at each end, shown in Fig. 8b, for a height of about 6 in. (150 mm) above the foundation. This damage was essentially cosmetic and could have been easily repaired without disrupting the normal operations of the building.

Minor cracking was developed at the base of all columns, but it was clear from the small width of these cracks that no yielding of reinforcement in the columns had occurred.

Fig. 8c shows the crack pattern at the base of an external gravity load column at the end of testing in the wall direction. The only other damage observed was hairline cracks in the floor systems, particularly in the cast-in-place topping above the joints between the hollow-core slabs.

Force-Displacement Characteristics — It is impossible within the space limitations of this paper to provide the results for all of the tests carried out in the two directions of loading. As a consequence, only the most important tests will be discussed. However, the displacement profiles up the height of the building at the peak roof displacement for different levels

Fig. 8.
Damage to building
after testing to
1.5xZone 4 intensity.



of input excitation in the wall direction are shown in Fig. 9.

These results provide some indication of the nonlinear relationship between excitation intensity and peak displacement. For example, at EQ1 excitation, the intensity was 33 percent of the design level, but the roof level displacement was only 14.7 percent of that recorded under EQ3, the design level event.

Initial testing at the design level EQ3 had to be aborted after 1.0 seconds of scaled earthquake record because of unacceptably high floor force levels. Before resuming the testing, the earthquake record was filtered to reduce the severity of third to fifth mode effects. Analyses of the structure using models described subsequently in this paper confirmed that this filtering would not influence the peak displacements or base shear forces, which were primarily influenced by the first (inelastic) and second modes of response.

The measured displacement response of the building in the wall direction to 1.5xZone 4 (i.e., 1.5xEQ3 input) is shown in Fig. 10. Displacements for each floor level are plotted against time, where the time is based on the input accelerogram time scale, and needs to be divided by 0.6 to provide prototype time.

The displacement response appears to be dominated by first mode deformation patterns, with displacements at different floor levels approximately proportional to the height at all times. However, examination of the story shear force time-history response for the same test, shown in Fig. 11, indicates that there was a considerable amount of higher mode response, particularly in the earlier part of the record. During the maximum displacement response pulse, the force response is closer to that expected of the first inelastic mode.

This difference in sensitivity to higher modes between the displacement and force response is to be expected, since only the first mode is significantly modified by ductility. Higher modes remain elastic and the displacement response for these modes is very small because of their large stiffness. It should be noted that peak

shear forces for the lower floors of the building occur in the early stages of response, not when the structure reached the peak lateral displacement.

The overall hysteretic characteristics of the building in the wall direction are best illustrated by the base moment/roof-level displacement hysteresis response. Two examples are given for the wall direction in Figs. 12 and 13, respectively.

The first example (see Fig. 12) plots the response under the inverted triangle excitation carried out to the peak displacement response obtained during the EQ3 design-level input. This enables the shape, stability and symmetry of the response to be observed. It will be noted that the energy dissipated by the wall is considerable, and that equal strength was obtained in both directions of response.

Fig. 13 shows the moment-displacement response obtained during the final test in the wall direction, namely, the pseudodynamic test to 1.5xEQ3 (1.5x Zone 4). The shape of the hysteretic response is now much more irregular than for the inverted triangle test, but the high level of energy dissipation is still apparent. The low residual drift at the end of testing is identified by the large solid circle.

It is of interest to examine the envelopes, with height, of various actions developed in the wall. To this end, Fig. 14 compares the envelopes of story overturning moment, story shear force, and floor forces obtained from testing the building at the EQ3 design level. In this arrangement, the envelopes correspond to the design inverted triangular distribution of forces. The floor forces represent the actual force levels applied to the floors by the two actuators at each floor level.

The increase in the maximum recorded base moment over the design level (see Fig. 14a), of approximately 25 percent, represents the overstrength resulting from the U-shaped energy dissipators having higher strength than the design value; and also, to a lesser extent, due to lateral resistance provided by the columns of the building, which were ignored in the design approach.

At levels above the base, it will be observed that the experimental distri-

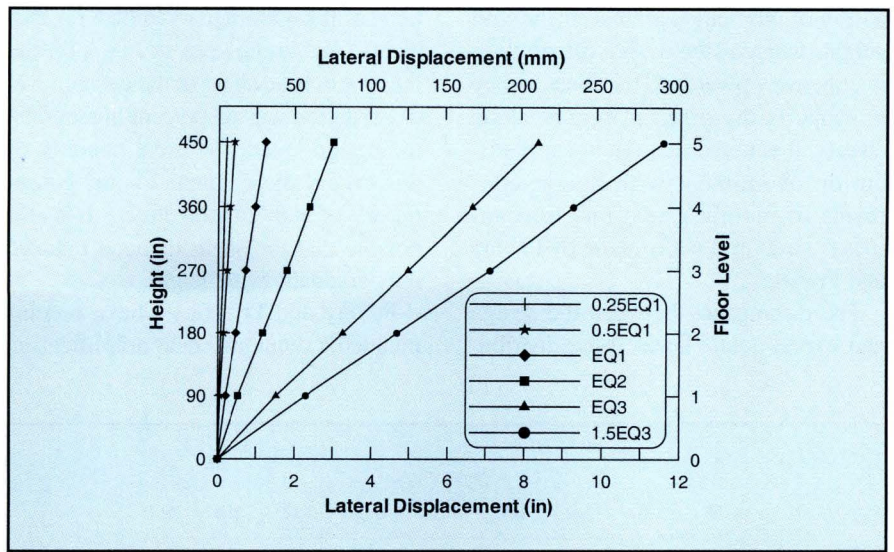


Fig. 9. Peak displacement profiles up the wall at different levels of seismic excitation.

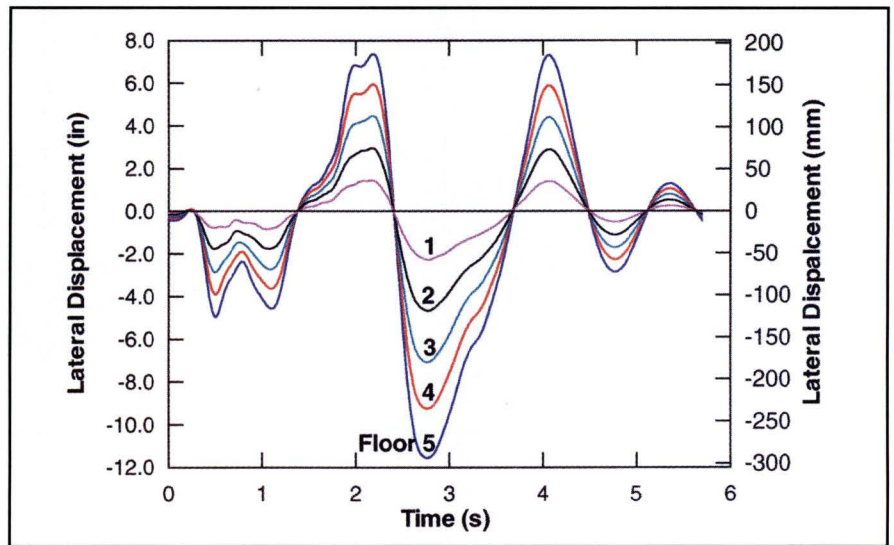


Fig. 10. Time-history of wall direction displacement response to 1.5xZone 4 excitation.

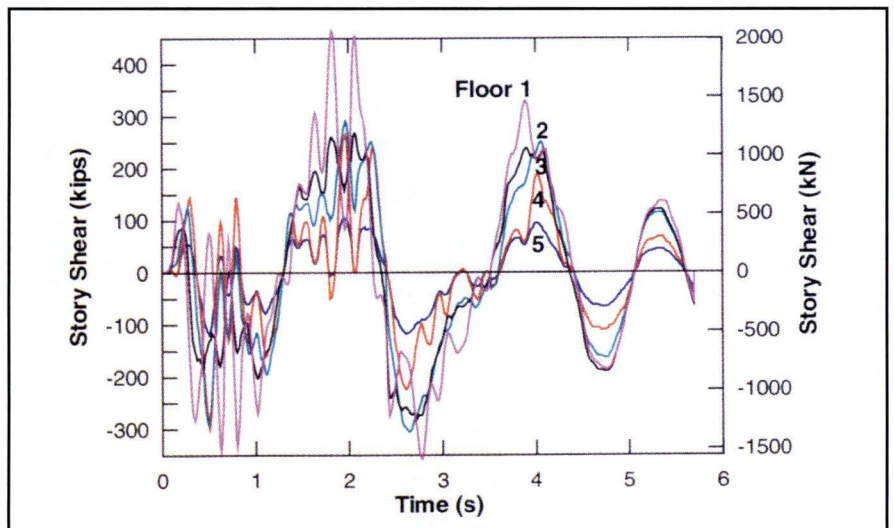


Fig. 11. Time-history of wall direction story shear force response to 1.5xZone 4 excitation.

bution of moment is almost linear with height, whereas the design distribution is concave upwards. This discrepancy in shape is the result of higher mode effects. It is noted that the linear distribution of moment with height conforms to recommendations for cantilever structural walls made by Paulay and Priestley.¹¹

The discrepancy between the design and experimental shear force distribu-

tions is much more marked than for moments. As can be seen in Fig. 14b, the maximum base shear at the design level of excitation was 63 percent higher than the design level. The great majority of this excess shear demand is the consequence of higher mode effects. It is also notable that the shear demand reduced only gradually with height.

Paulay and Priestley¹¹ have recommended a dynamic shear amplification

for a five-story cantilever wall structure of 40 percent to account for higher mode effects. This shows a reasonable agreement with the experimental value, when the overstrength due to flexural enhancement, apparent in Fig. 14a, is included.

The biggest differences between experiment and design levels were in the floor force levels. As seen in Fig. 14c, the floor force levels greatly exceeded the design values at all heights of the building. It is also clear that the floor forces do not show any tendency to reduce in the lower levels, as would be expected from a predominantly first mode response. For the wall direction of response, a rough approximation to the floor force levels for design purposes would be to apply 75 percent of the design base shear as a floor force at each level.

Note that these high floor force levels, while not significantly influencing the moment demand at the base, are important since they represent the magnitude of diaphragm forces that must be transmitted from floors to lateral force-resisting elements. These high force levels caused considerable problems in the testing of the PRESS building.

Recognizing the potential impact of higher mode effects, Ms. Suzanne Nakaki and Professor John Stanton, the building designers,² had designed all diaphragm-to-wall and diaphragm-to-frame connections for force levels corresponding to 50 percent higher than the top story design level. Actuator connections to the floors were designed for the same force levels.

In the test, the design ultimate strength of these actuator connections was exceeded by up to 44 percent, and significant yielding of the connections occurred. Without material overstrength in the connections, failure would have occurred. However, as a consequence of the unexpectedly high floor forces, it was necessary to provide extra damping to the fourth and fifth modes in the pseudodynamic test control. Without this extra damping, floor forces would have been even higher.

It is possible that a part of the higher mode effects resulted from the iteration procedure used to impose the cal-

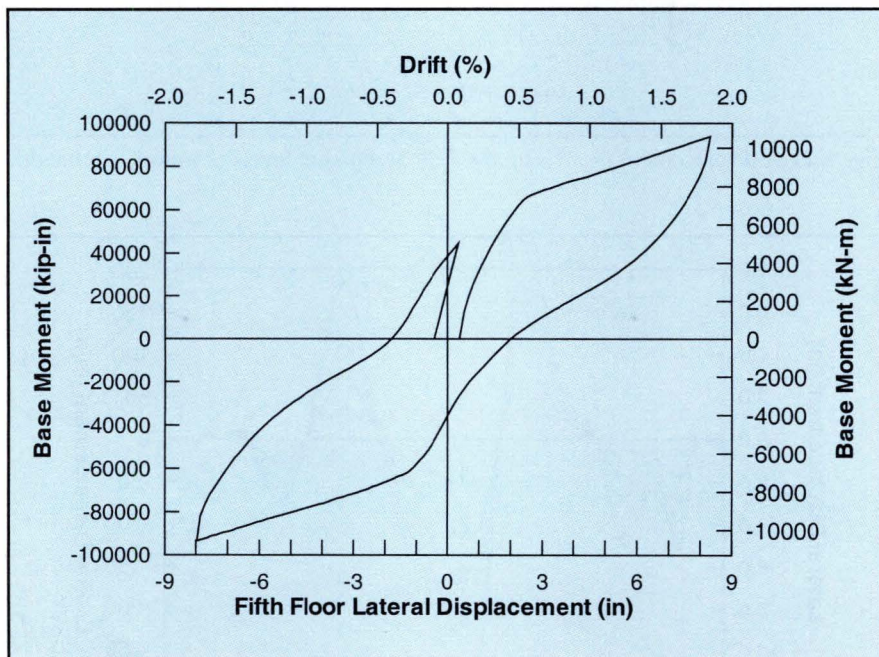


Fig. 12. Wall base-moment/roof-level displacement hysteresis response to inverted triangular force input to 8.3 in. (211 mm) peak displacement.

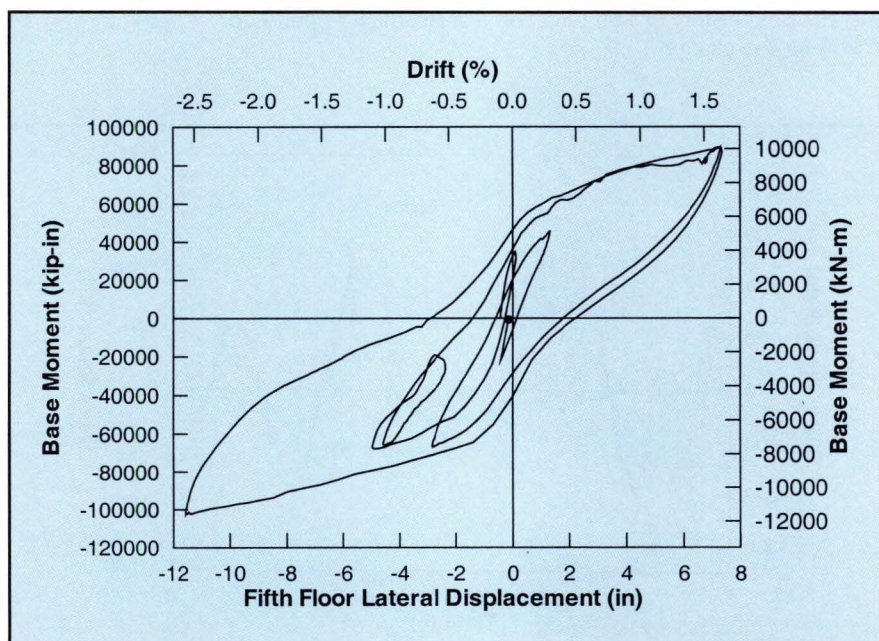


Fig. 13. Wall base-moment/roof-level displacement hysteresis response to 1.5xZone 4 excitation.

culated displacements at each time step, discussed previously. However, a comparison with analytical results indicated that similar levels of higher mode effects were predicted. Further, as noted above, the floor forces were reduced in the pseudodynamic tests by applying extra damping to the higher modes. It is clear that current American design practice does not adequately consider the influence of higher mode effects.

As a consequence of the negligible damage and the very low residual drift, it was apparent that after being subjected to an earthquake 50 percent higher than the design intensity, the building had responded within the serviceability or "immediate occupancy" level of performance defined in Ref. 6.

Frame Direction of Response

General Observations — Response of the building in the early stages of loading was characterized by low levels of damage, with all inelastic action occurring in the beam-to-column connections, as intended. Minor flexural cracking was noted in the beams of the TCY frame at locations other than the beam-column interfaces, and minor shear cracking of the beam-to-column joints was noted on testing to EQ2, corresponding to 50 percent of the design intensity. This joint cracking was much more apparent in the non-prestressed frame than the prestressed frame, and was more noticeable in external columns when subjected to seismic axial tension than axial compression.

At EQ2, incipient spalling was noted at the base of the beams of the TCY-gap connections where they were connected to the columns, as was a slight tendency for the beams to slide up the column interface.

During testing to EQ3, the design level of ground motion, it was observed that the beams of the hybrid frames experienced some inward rotation about their longitudinal axes. This torsional rotation and the cause of the rotation are illustrated in Fig. 15. The heavy double-tee floor members were hung off the side of the beams at the lower three floors, causing a torsional moment of significant magnitude. Under inelastic action, the torsion in the hybrid beams was primarily re-

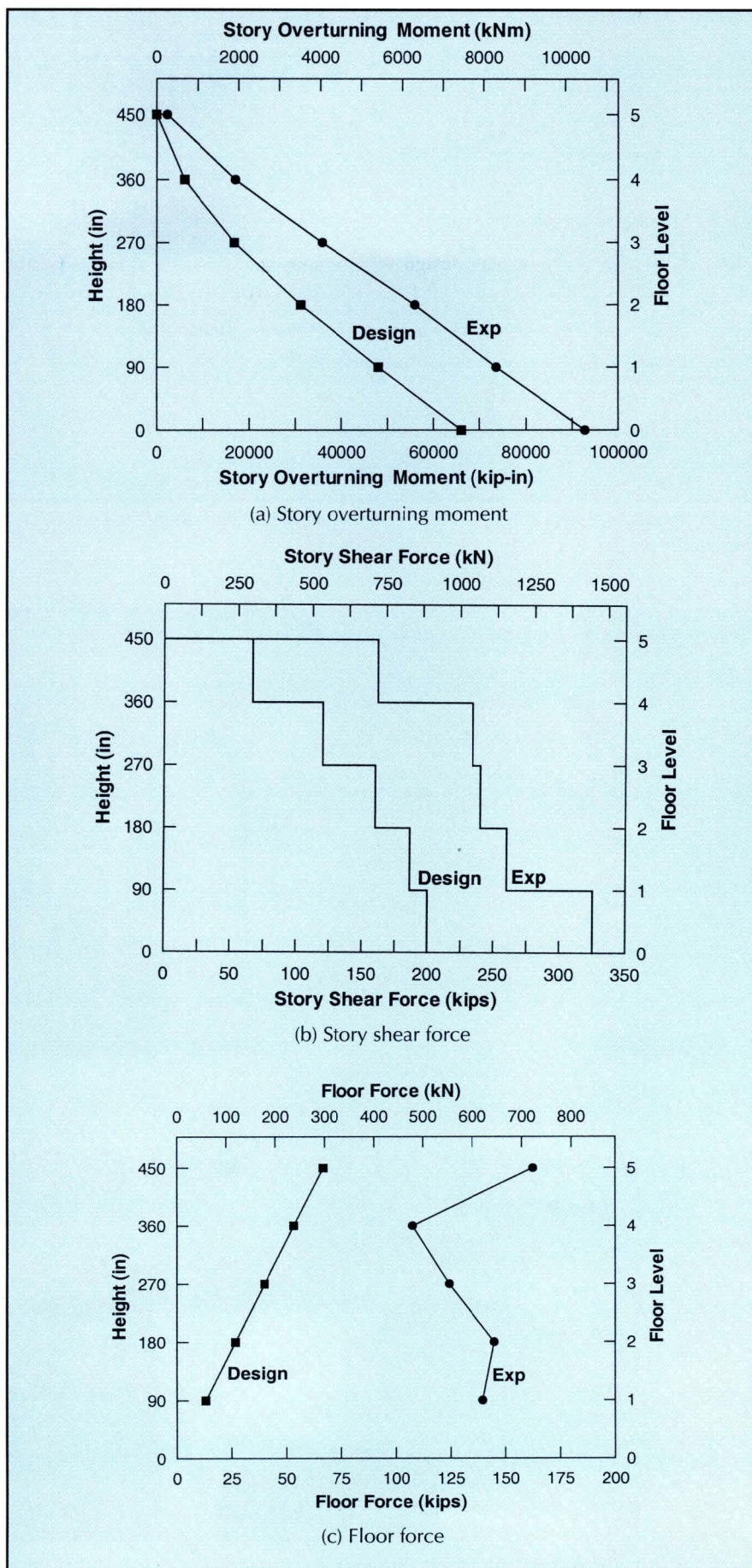


Fig. 14. Comparison of design and experiment force envelopes at design level (Zone 4) excitation.

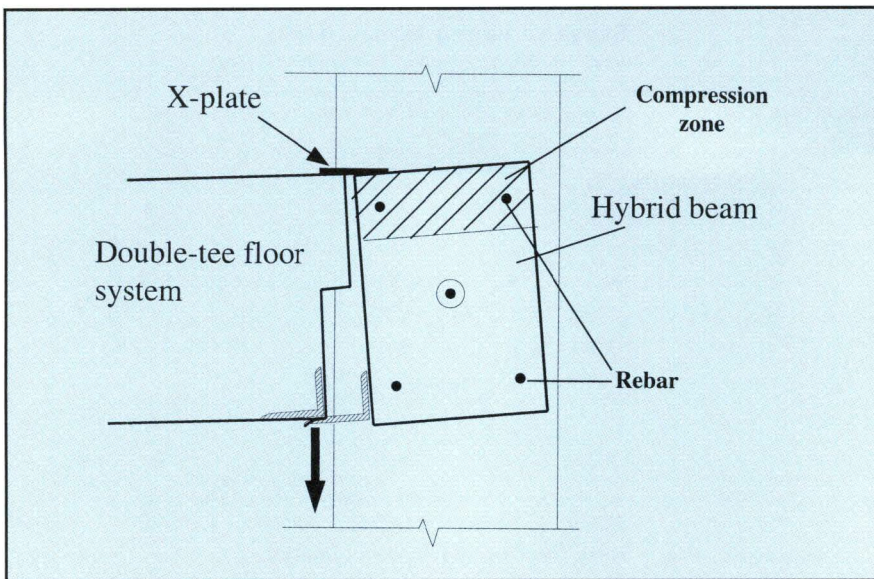


Fig. 15. Rotation of hybrid beam due to connection detail with double-tee floor member.

sisted by the compression zone at the beam-column interface, with a small contribution from dowel action of the mild steel damping bars crossing the interface.

The torsional resistance of these actions was insufficient to prevent the rotation at the lower three floors of the prestressed frame. The very high floor force levels also exacerbated the problem since these provided additional vertical forces to the floors, which in one direction of response more than doubled the reactions of the double tees on the prestressed beams, and hence increasing the torsion by a similar amount.

Following testing at EQ3 input, the steel base of the floor beams was welded to the brackets on the side of

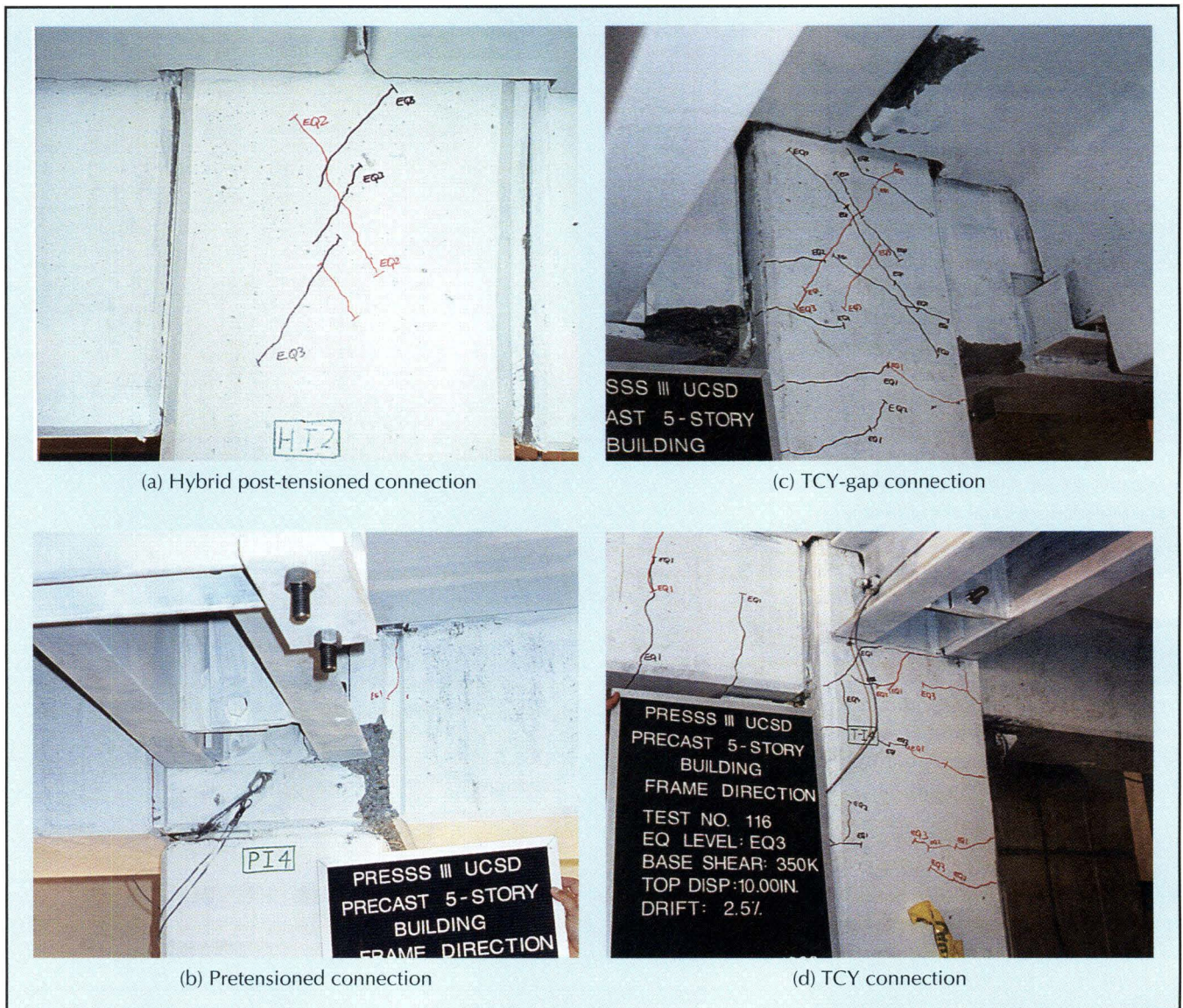


Fig. 16. Condition of frame connections after design level of response.

the prestressed beams, effectively locking in the rotation at the existing level, and prohibiting further rotation. It is clear that support of these heavy double-tee floor members should be provided as close to the beam centerline as possible to reduce the torsional effect, which would be important whether the frame was precast or cast in place.

It should also be noted that although the test building was subjected to additional forces from the actuator reactions, as noted above, the actual dead load reactions were less than in the prototype building because of the scale factor involved. Calculations showed that the total reaction in the test building was similar to that to be expected in practice. De-

spite continuing the test with the hybrid beams having a locked-in torsional rotation of more than 3 degrees, there were no visible signs of this influencing the response.

On testing the frame with the hybrid beams under the design level EQ3 input, a maximum roof-level displacement of 10 in. (254 mm) was sustained, corresponding to an average peak drift 10 percent higher than the design level of 2 percent, although local interstory drifts were higher. Again, this is seen to be a good verification of the displacement-based design procedure. It is believed that the slightly larger than expected drift was a consequence of effective damping levels being somewhat less than those assumed in the design.

Fig. 16 shows the condition of typical frame connections after subjecting the building to the EQ3 design level input, and two subsequent cycles of inverted triangle testing to the same peak displacement sustained in the pseudodynamic test. As is clear from Fig. 16a, the hybrid prestressed connections exhibited little or no damage at this stage, despite the torsional rotation noted above. Joint cracking was minor, with maximum crack widths of about 0.005 in. (0.12 mm). Very little cracking had developed in the beams except at the connection to the column.

Similarly, excellent behavior was exhibited by the pretensioned connections provided at the upper two levels of the prestressed frame (see Fig.

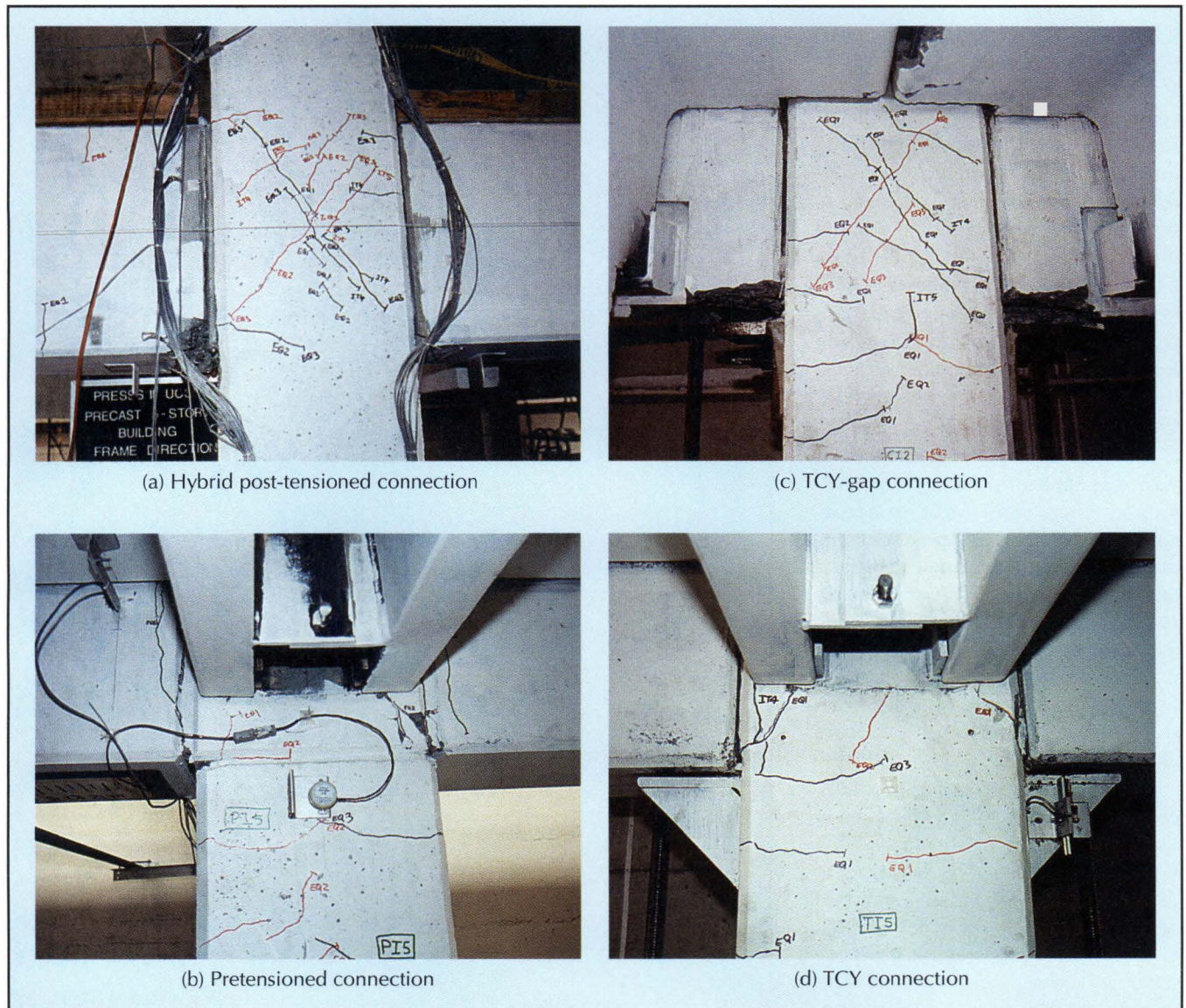


Fig. 17. Condition of frame connections after being subjected to drift levels more than twice design level.

16b). The inelastic action for these connectors was concentrated in single cracks that developed at or near the reveals formed in the beams in line with the column faces. Joint cracking in the pretensioned connections was less apparent than at the hybrid connections provided at the lower three levels. At the design stage of seismic response, no repair would have been needed to the prestressed frame.

Fig. 16c shows the condition of a typical interior TCY-gap connection after the design level excitation. It is to be noted that there is significant spalling from the soffit of the beams immediately adjacent to the connection. Also, there is some crushing and deterioration of the fiber-grout pad at the base of the gap. It had been observed during testing to this level that there was upwards sliding of the beams on the grout pads during maximum response levels.

Analysis showed that this was the consequence of an insufficient clamping force in the post-tensioned threaded bars at the base of the connection. These bars had been sized to provide a sufficient clamping force to resist the anticipated shear at the beam interface when the top mild steel connection bars yielded in compression. Under this condition, the clamping force across the grout pad is reduced by an amount equal to the top reinforcing bar compressive force.

Although an overstrength factor of 1.25 was applied to the top compressive nominal yield force in accordance with American practice, this did not provide an accurate representation of the actual overstrength resulting from yield strength exceeding the nominal minimum value, coupled with the strength increase resulting from strain hardening. In actual practice, higher overstrength factors should be provided.

The condition of the upper TCY connections was good, as illustrated in Fig. 16d, this despite the observation that incipient sliding was occurring at the interface. It should be emphasized that this sliding or shear deformation in the plastic hinge region has been commonly observed in tests of reinforced concrete beam-to-column connections at moderate ductility levels.

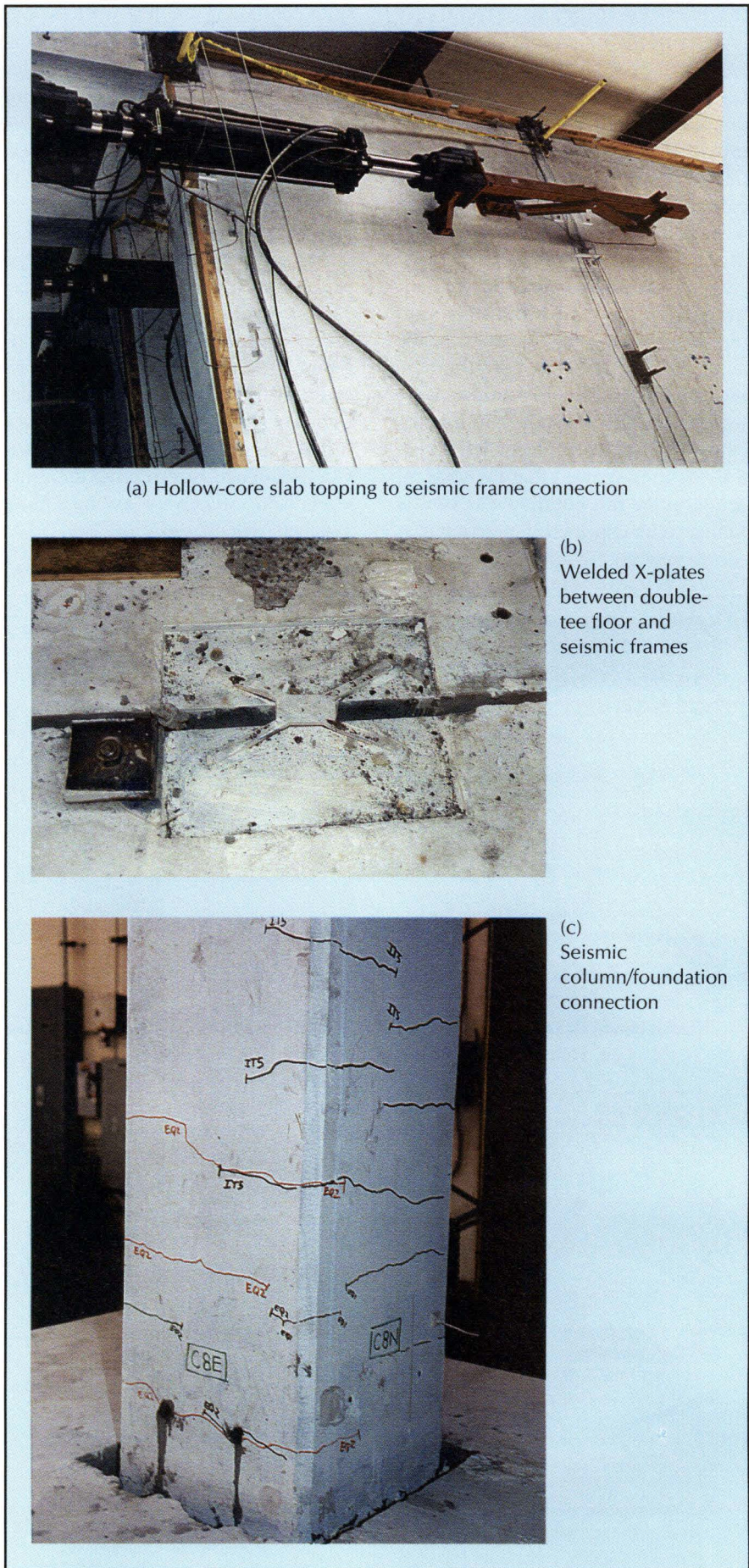


Fig. 18. Condition of various structural elements at end of testing.

Fig. 17 shows the condition of the various connections after cycling to more than twice the design level drifts. The hybrid prestressed connections (see Fig. 17a) were performing extremely well at this stage, with only minor damage in the form of cover spalling, and some crushing and incipient break-down of the fiber grout pads between the beams and columns. No significant increase in width of the joint shear cracks above that sustained at the design level was observed. It is probable that the joint strain gauge results will show that substantial reductions in joint reinforcement will be possible with this detail.

The performance of the pretensioned connections in the upper floors of the prestressed frame was also excellent, as shown in Fig. 17b. Damage in these connections was also limited to superficial cover spalling at, or adjacent to the beam-column interface.

Sliding of the TCY-gap connections had continued during testing levels above the design level. As a consequence of the high tension strains from the seismic response coupled with the dowel bending caused by the interface sliding, a few of the mild steel reinforcing bars crossing the interfaces fractured in the latter stages of testing. It is clear that sliding of the TCY-gap beams could have been avoided if the clamping force provided by the post-tensioned threaded bars at the base of the beams had been higher.

It was also observed that early crushing of the cover concrete may be inevitable with this design detail because of the high compressive force across the grout pad when the top bars are in tension. Strengthening the beam ends or some other detail to inhibit crushing may be advisable in future designs.

Fig. 17c shows the condition of a typical TCY-gap interior-column connection at the end of testing. Damage is still much less than would be expected from a conventional reinforced concrete beam-to-column joint at this level of drift. Design recommendations for improving this detail will follow in a subsequent paper.

Damage to the TCY connections in the upper levels of the reinforced concrete frame was not significantly dif-

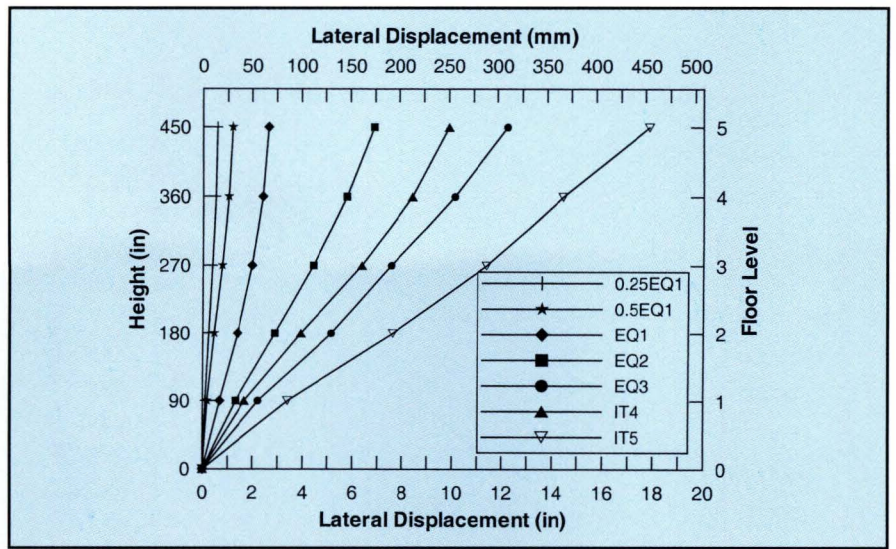


Fig. 19. Peak displacement profiles up the frames at different levels of seismic excitation.

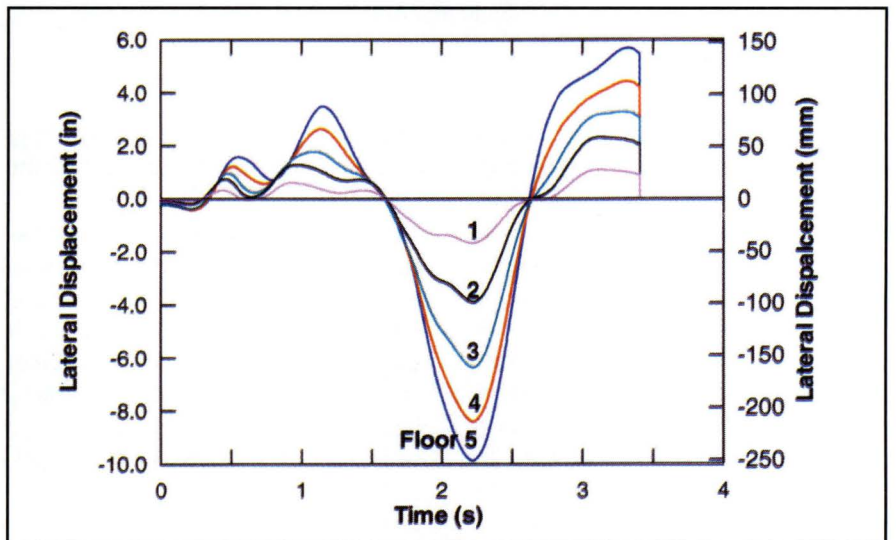


Fig. 20. Time-history of frame direction displacement response to Zone 4 excitation.

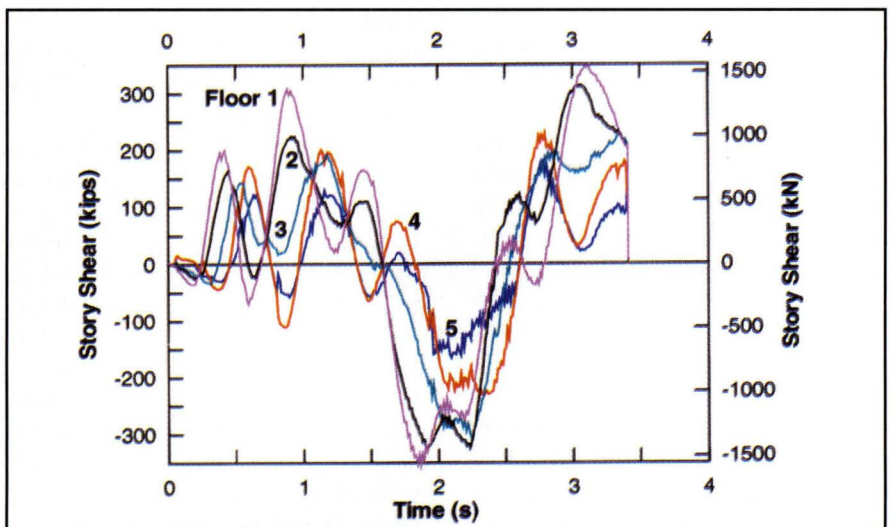


Fig. 21 Time-history of frame direction story shear force response to Zone 4 excitation.

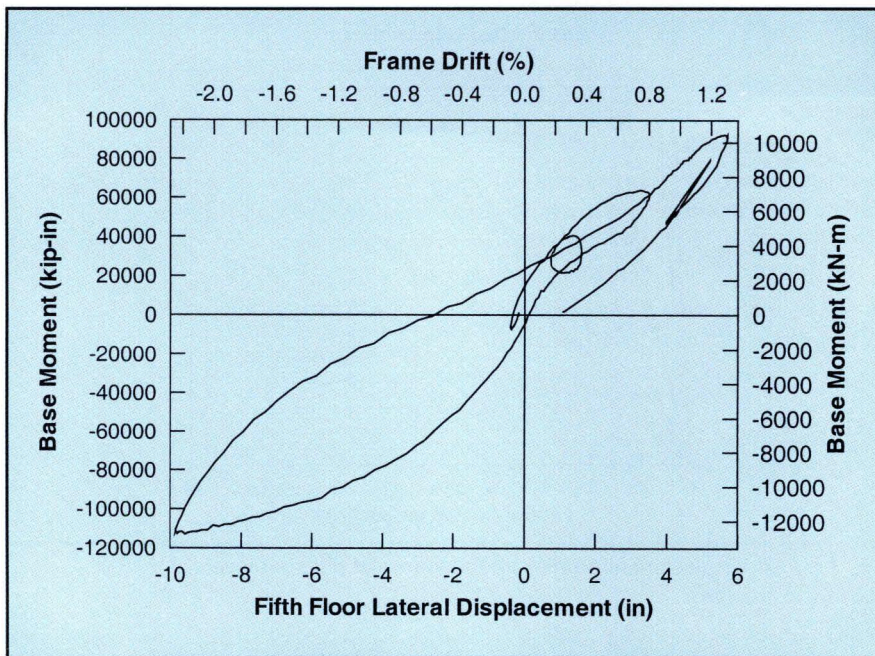


Fig. 22. Frame direction gross base-moment/roof-level displacement hysteresis response to Zone 4 excitation.

ferent from that at the design level. A small amount of interface sliding continued to occur at these higher levels of response, but crack patterns and spalling did not noticeably change. Some loss of bond between the top level reinforcing bar in the grout ducts was noted at the exterior connections, with the headed reinforcing bar, which were exposed at the ends of the connection being pushed out by up to 1 in. (25 mm). There did not appear to be any significant strength reduction associated with this action. Fig. 17d shows the condition of a typical TCY connection at the end of testing.

The condition of selected other structural elements at the end of the test program is shown in Fig. 18. The connection detail between the cast-in-place hollow-core topping and the frames, formed by drag bars from the topping connecting into pockets in the top of the frame beams, shown in Fig. 18a, performed very well. There was only minor cracking along the interface, despite the very high levels of floor forces.

The welded X-plate connectors between the double-tee floor members and the frame beams also performed well, although these exhibited significant inelastic action and permanent distortion, as illustrated in Fig. 18b. Damage to the column bases was min-

imal, with very minor spalling being observed at some, but not all of the seismic columns (see Fig. 18c).

Force-Displacement Characteristics — Peak displacement profiles up the frames at different levels of seismic excitation are plotted in Fig. 19. It will be noted that despite the different characteristics, particularly relating to initial stiffness of the two frames, and to a lesser extent, relating to strength, the test procedure ensured that the two frames were subjected to the same displacement at all times. The displacement profiles show a pronounced curvature, with reduction in drift at the upper stories, particularly in the early stages of testing. This is believed to be a consequence of the excess strength provided at the upper levels.

Time histories of displacement response and story shear force at different levels of the building are shown in Figs. 20 and 21, respectively, under the EQ3 design level of response. This test ended slightly prematurely due to excessive story force levels, despite filtering the earthquake record, as discussed earlier. However, at this stage, the peak displacement response had already occurred and the record was within 0.5 seconds of entering the free decay section of input, i.e., the input record had a trailing section of zero acceleration to enable free decay to be

observed. The abrupt termination of the record is apparent in both Figs. 20 and 21.

The story shear force plots represent the sum of the shear force in the two frames. It will be observed that a very significant higher mode response is particularly apparent in the early stages of the story shear forces, but is much less apparent in the displacement response, or during the peak displacement pulse, as was observed for the shear wall direction of testing.

The gross base moment/roof displacement hysteresis response recorded during the EQ3 response is plotted in Fig. 22. The moment here is the overturning moment found from the sum of the response of the two frames. It will be noted that although significant energy dissipation is apparent in Fig. 22, it is somewhat less than that for the wall direction of response.

In Fig. 23, the hysteretic base moment/roof displacement response under the inverted triangle loading to 12.2 and 17.9 in. (310 and 454 mm) peak displacements is plotted with the response of the two frames being separated. Since two actuators applied the lateral forces at each level, with one actuator adjacent to each frame, and since the torsional resistance provided by the central wall was insignificant, the determination of the forces carried by each frame was straightforward.

It will be noted that the peak moments sustained by the two frames were very similar, but that the hysteretic response of the frames was very different, with the non-prestressed frame exhibiting more energy dissipation, and more residual displacement than the prestressed frame, as was expected. The lack of significant strength reduction on testing through two complete cycles at the lower displacements of Fig. 23 is apparent.

On the second cycle to peak displacement at 17.9 in. (454 mm), the test control system developed a severe instability resulting in the building being subjected to violent shaking, and an emergency shut-down occurred. Although this instability, which was electronic, rather than structural, did not appear to induce any further damage to the building, the test program was terminated at this stage.

Fig. 24 plots the envelopes of overturning moment, story shear force, and story force levels as functions of height, for the EQ3 design level earthquake, and compares them with the design envelopes. Trends apparent in Fig. 24 are similar to those for the wall direction of response (see Fig. 14), although the extent of overstrength is less, particularly for overturning moments and story shear. To some extent this can be attributed to the strength reduction of the TCY-gap connections due to premature spalling and interface sliding, which was noted earlier.

ANALYTICAL MODELING OF RESPONSE

Prime responsibility for the analytical modeling of the building rests with a research team from Lehigh University, who will be reporting separately on experiment versus prediction comparisons at a later date. Their modeling has been based on fiber-element representation of the various structural components. However, as part of the test control, it was necessary to have the ability to predict the response of the building prior to performing pseudodynamic tests.

To this end, simple models were developed to represent the wall and frame directions of response, based on one-dimensional inelastic elements whose properties were based on section analyses. Essentially, these were typical design-level representations of the building.

Wall Direction Model

The analytical model for the wall direction response prediction is shown in Fig. 25. The two walls were separately represented by elements at their center-lines and given structural properties based on the uncracked section. The walls were supported at the base on rigid horizontal beams supported at each end by compression-only springs located at the calculated position of the center of compression at each wall end under rocking response. Properties of these springs are indicated in Fig. 25.

As shown in Fig. 25, the springs were preloaded by forces representing the gravity weight and unbonded prestressing force at the wall base. As the wall rocks, the unbonded prestressing threaded bars extend, resulting in an increased clamping force at the base. This was modeled by an additional spring directly under the wall element, as shown in Fig. 25.

The two wall elements were connected by vertical springs acting between rigid horizontal links extending at each floor level. These inelastic springs represented the characteristics of the U-shaped flexural yielding energy dissipators connecting the wall, which are apparent in Fig. 3. The properties for these springs were determined by testing spare dissipators prior to the building test. It should be mentioned that any additional strength and stiffness in the wall direction resulting from column stiffness were ignored in the analysis.

This simple model enabled realistic estimates of the force displacement response to be obtained prior to testing. Prior to each earthquake record being imposed on the test building, an inelastic time-history analysis was run on the analytical model using the Ruaukoko computer program.¹² Thus, the results from these analyses were true predictions (rather than post-dictions) of response. No modification of

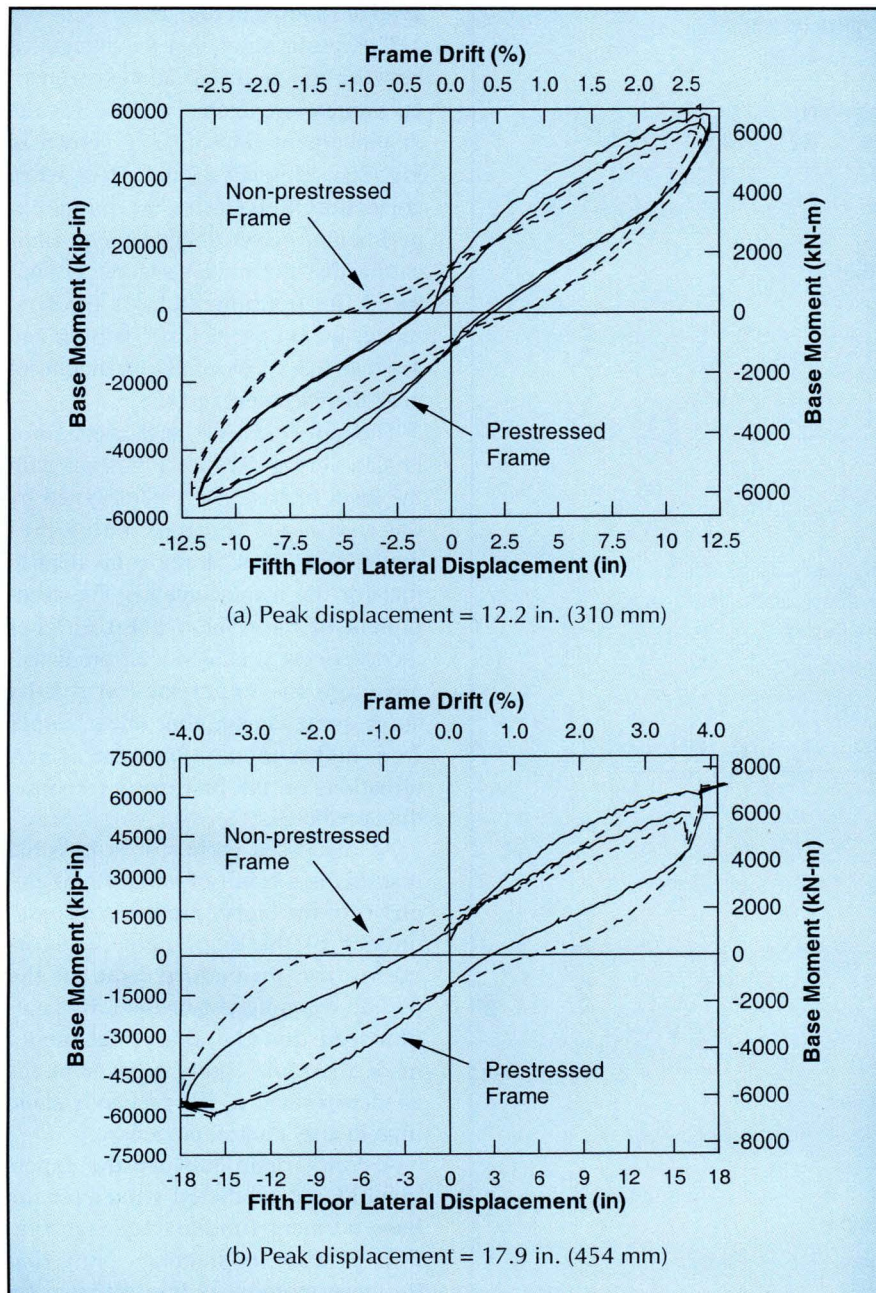


Fig. 23. Frame base-moment/roof-level displacement hysteresis response to inverse triangle loading.

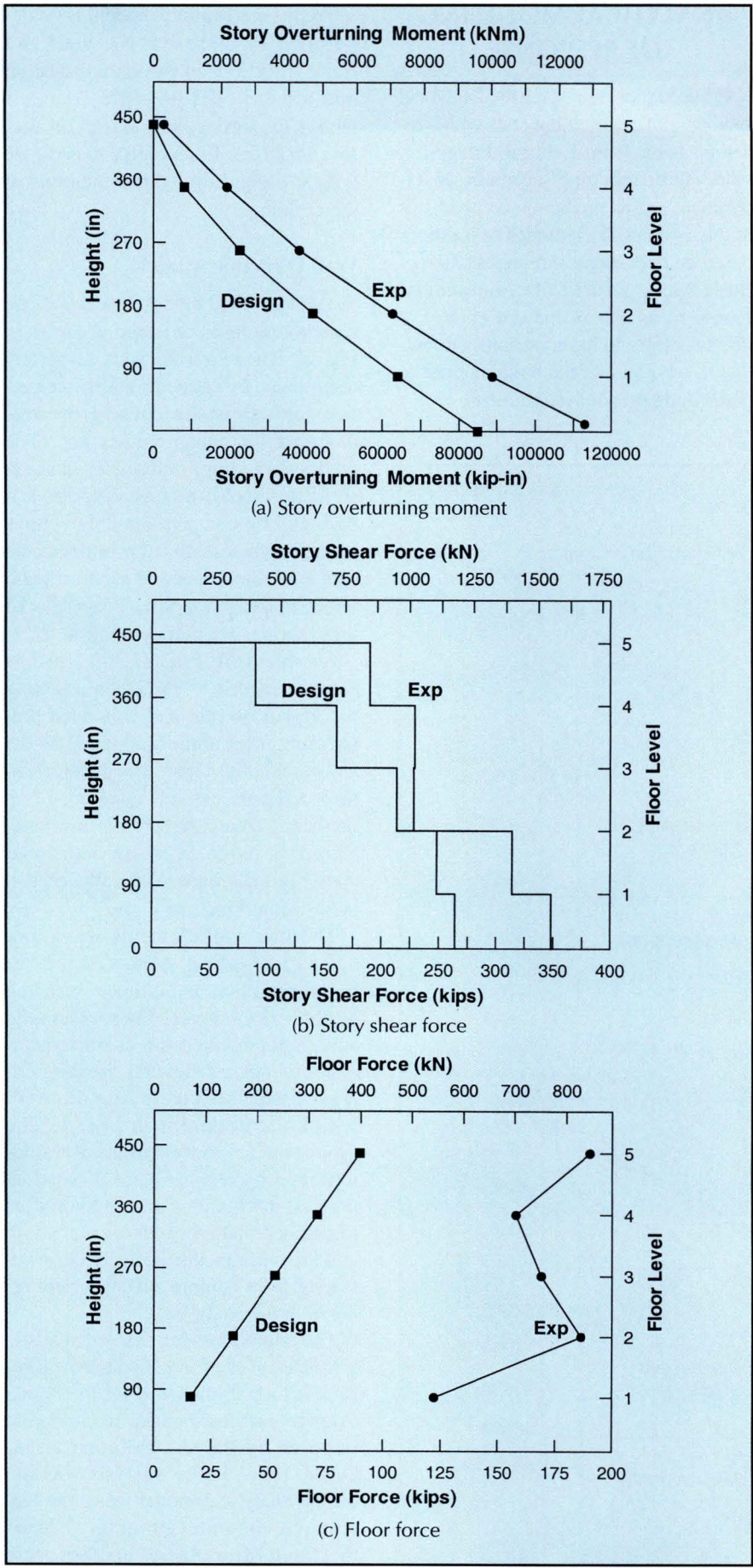


Fig. 24. Comparison of design and experiment force envelopes at design level (Zone 4) excitation.

the analytical model was made after the test program started.

Wall Direction Prediction and Experiment Comparisons

Space limitations do not permit more than a limited comparison between the analytical predictions and the experimental results. A full description of the analytical model details and analysis results will shortly be available from UCSD.⁸ A comparison of the predicted and observed time histories of roof-level displacement, base shear force, and base moment for the 1.5EQ3 maximum response level are shown in Fig. 26.

The results show that the agreement between the predicted and experimental values is extremely close for the displacement time-history shown in Fig. 26a. This is especially true when correction is made for the initial experimental offset displacement, indicating that the model accurately captured the fundamentals of the first mode, including inelastic action, and was capable of excellent prediction of peak displacement response.

The agreement for base shear force is also very good (see Fig. 26b) with the level of base shear contributed by the first mode response being predicted with an accuracy equivalent to that for the displacements. The component of base shear due to higher mode effects was also well predicted, although the experimental results show somewhat higher shear forces from higher modes, apparent as perturbations on the first mode response, than predicted.

As discussed earlier, it is possible that this is a result of an artificial emphasis of the higher modes as a consequence of the displacement error-correction procedure used in the pseudo-dynamic test method. It is emphasized that the analytical model made the same damping assumptions as incorporated in the pseudodynamic time-history control procedure.

A comparison between the experimental and predicted values for the base moment time-history (see Fig. 26c) is also satisfactory. Note that the base moment is less affected by higher mode effects than is the base shear force. It is clear, however,

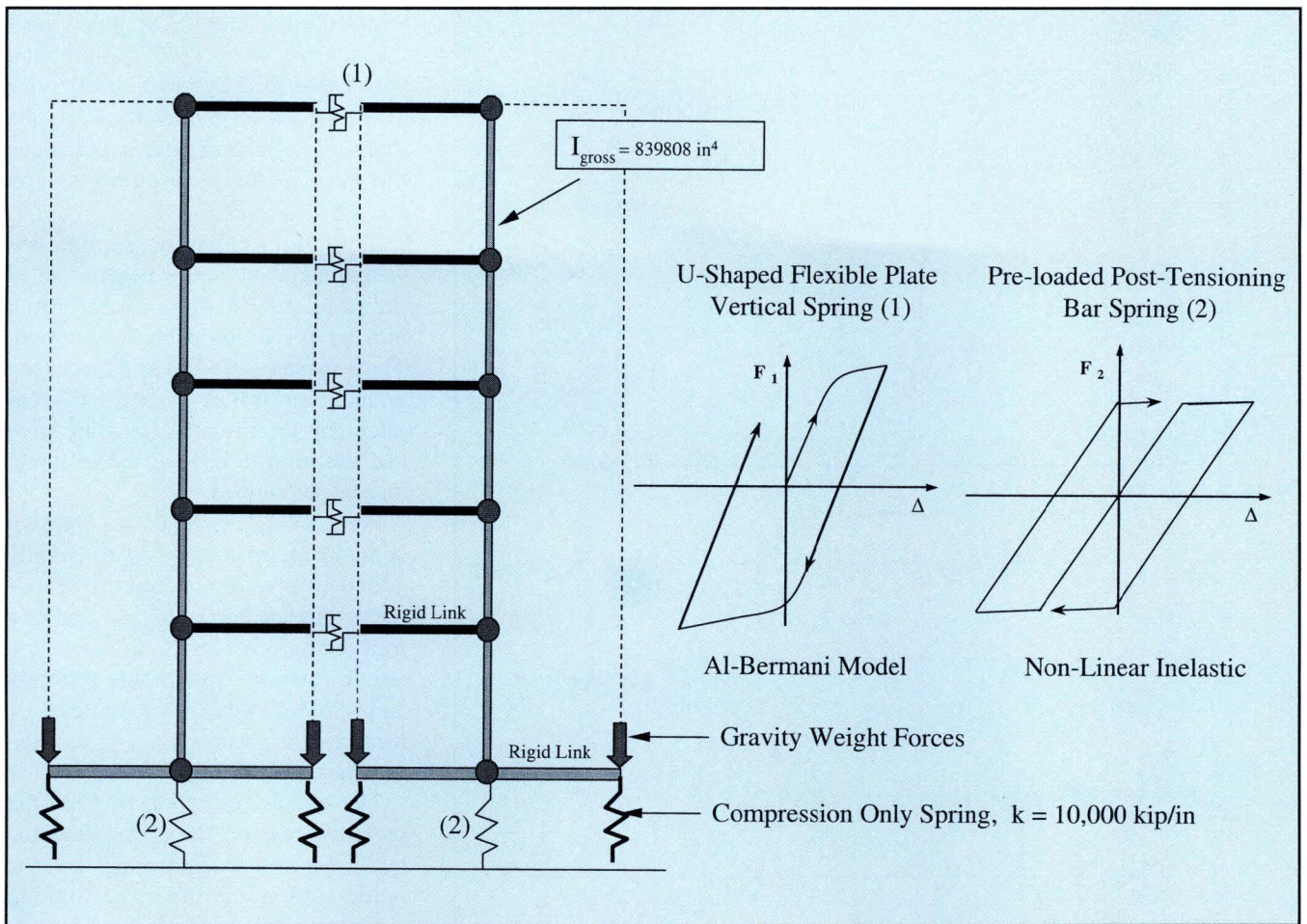


Fig. 25. Analytical model for wall direction response prediction.

that the strength was underestimated by about 20 percent at peak response.

A final comparison between the experimental and predicted values is provided in the base moment/roof level displacement envelopes of Fig. 27. This figure includes the experimental results from the full test sequence and compares them with the analytical results from a pushover analysis of the building, using the simple analytical model.

It will be seen that the agreement is reasonably good, with experimental peak values tending to exceed the predicted envelope by up to 25 percent. The initial stiffness of the model is somewhat higher than the experimental value.

This will be partly due to the support conditions assumed for the model, which consisted of point supports close to the wall extremities (see Fig. 25), and also due to the fact that the floor level displacements in the test were measured on the floors rather

than on the wall. The analytical model assumed rigid diaphragm behavior for the floors, whereas there was a small but significant flexibility between the floors and the wall resulting from the connection details.

The strength increase apparent in Figs. 26 and 27 can be attributed to two causes. In the wall direction, the six seismic frame columns and the two gravity columns would have contributed a small but significant amount to the base moment capacity of the structure. This was ignored in the analytical model.

Also, it is expected that the prestress losses in the tendons providing post-tensioning to the wall elements was less than the design value, which was used in the predictions. The influence of these two effects is sufficient to explain the overstrength.

Overall, the agreement between the experimental and predicted results is believed to be extremely satisfactory, considering the simplicity of the analytical model.

Frame Direction Model

The analytical model for the frame direction of response consisted of two planar frames slaved to have the same displacement at each floor level. Again, all members were represented by one-dimensional elements. Since the inelastic response was only expected at the beam-to-column or column-to-foundation connections, the members were modeled by elastic elements, representing the appropriate stiffness.

For the prestressed frame, this meant using a gross-section stiffness for the beams and a cracked section stiffness for the columns. For the non-prestressed frame, beam stiffness was initially based on the gross-section, reducing to 35 percent of the gross-section stiffness after cracking. Inelastic action at the beam-column interfaces of both frames was represented by inelastic moment-rotation springs at the beam-column interfaces.

Fig. 28 illustrates the fundamentals of this modeling for a hybrid pre-

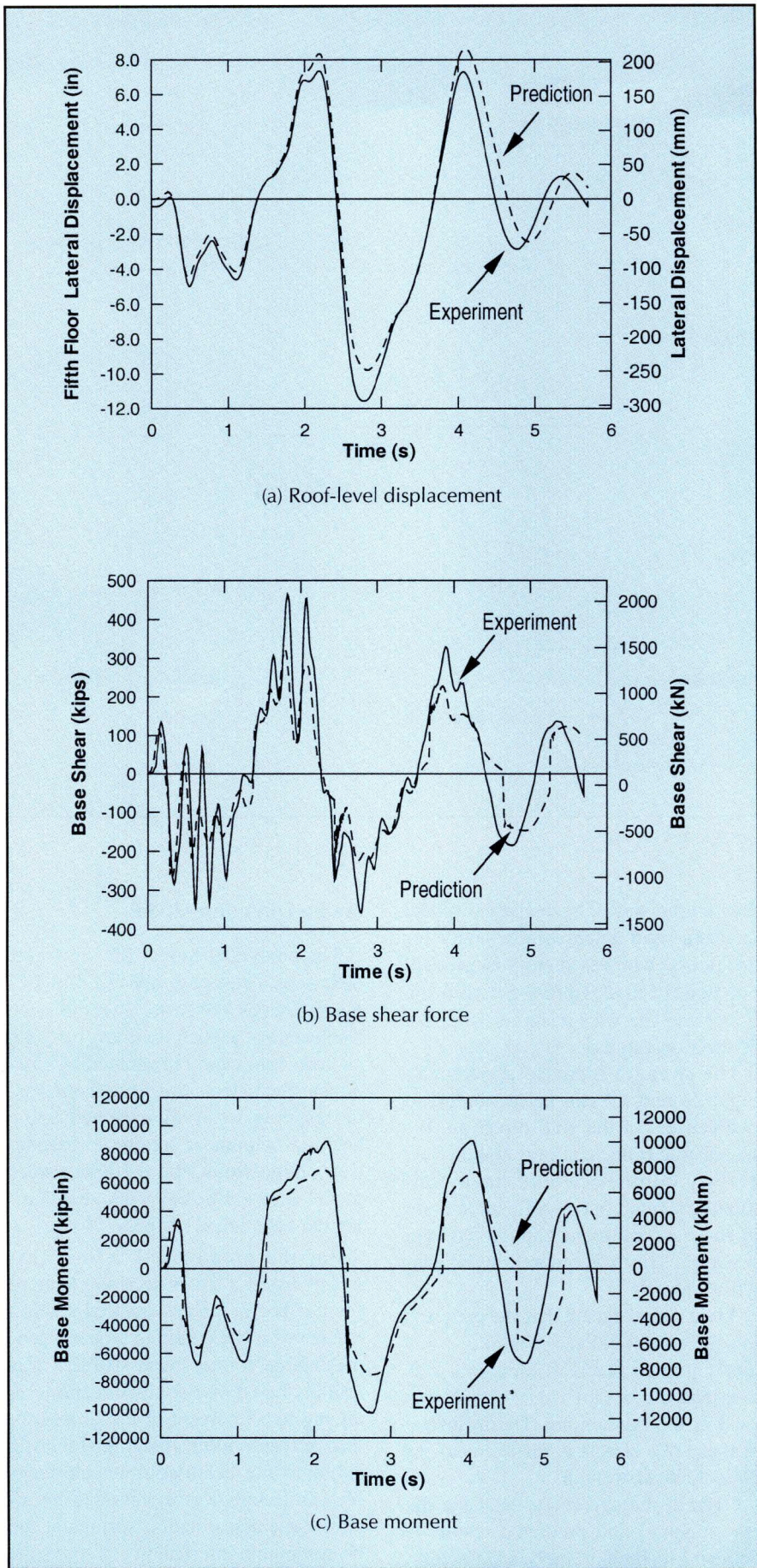


Fig. 26. Comparison of predicted and observed wall response at 1.5xZone 4 excitation.

stressed connection. The location of the centroid of concrete compression was established by hand calculations as a function of joint rotation. As the joint opened, the extension and hence the force of the prestressing tendon could be calculated.

Similarly, making appropriate assumptions about strain penetration of the mild steel damping reinforcing bar, its force could be determined. The separate relationships between moment and rotation provided separately by the prestress tension force and the reinforcing bar forces could thus be determined.

For a pushover analysis, the two components of moment were simply added to provide a composite moment-rotation curve. For an inelastic time-history analysis, separate hysteretic relationships for the prestress and reinforcing bar were modeled by using two inelastic springs in parallel, as indicated in Fig. 28.

The moment component from the prestress tension force was modeled by a nonlinear elastic spring (i.e., the model unloaded down the loading curve), without hysteretic energy dissipation. A Takeda degrading stiffness spring¹³ was used to model the moment component resulting from the yielding reinforcing bar.

The principles implied in Fig. 28 for the hybrid prestressed connection were applied, with modifications, to the other connection types. Thus, the moment-rotation behavior of the pre-tensioned connection at the upper levels of the prestressed frame was modeled solely by a nonlinear elastic spring, since there was no additional energy dissipation from mild steel reinforcing bars at these locations. Moment-rotation springs for the non-prestressed frame were modeled solely by Takeda degrading stiffness springs. Ruaumoko, the time history program used for the analyses contained both spring types within its extensive element library.

Frame Direction Prediction and Experiment Comparisons

Unlike the wall direction of response, the frame direction predictions were not calculated prior to testing the wall. Two rather minor modifications

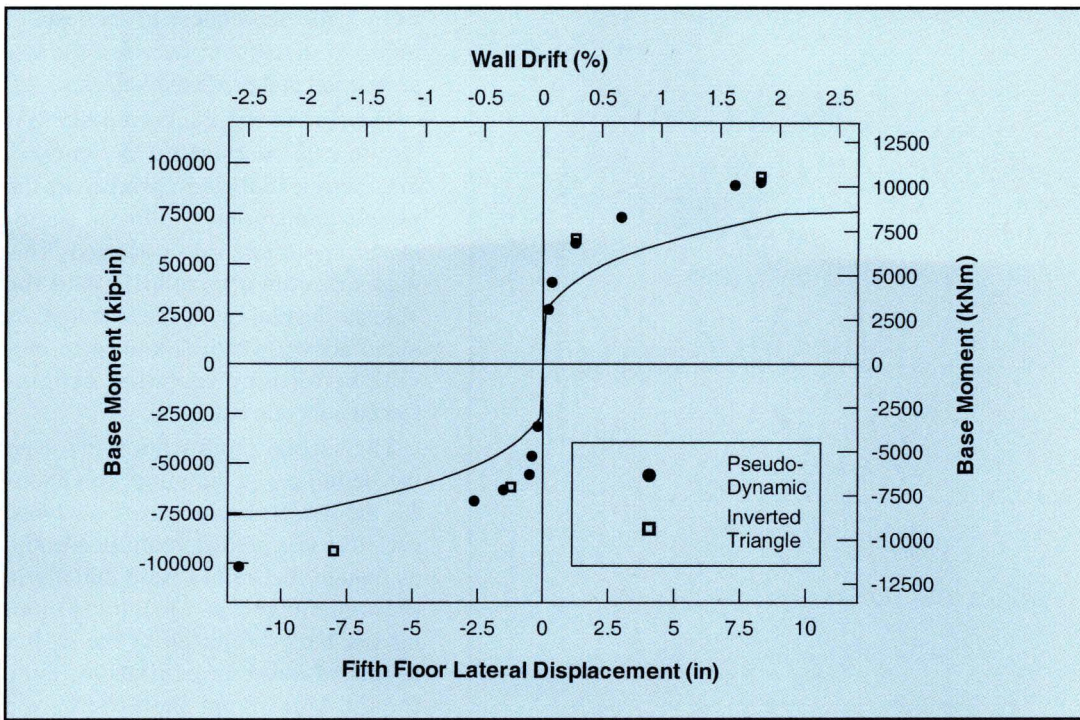


Fig. 27. Comparison of predicted and observed wall direction moment-displacement envelope response.

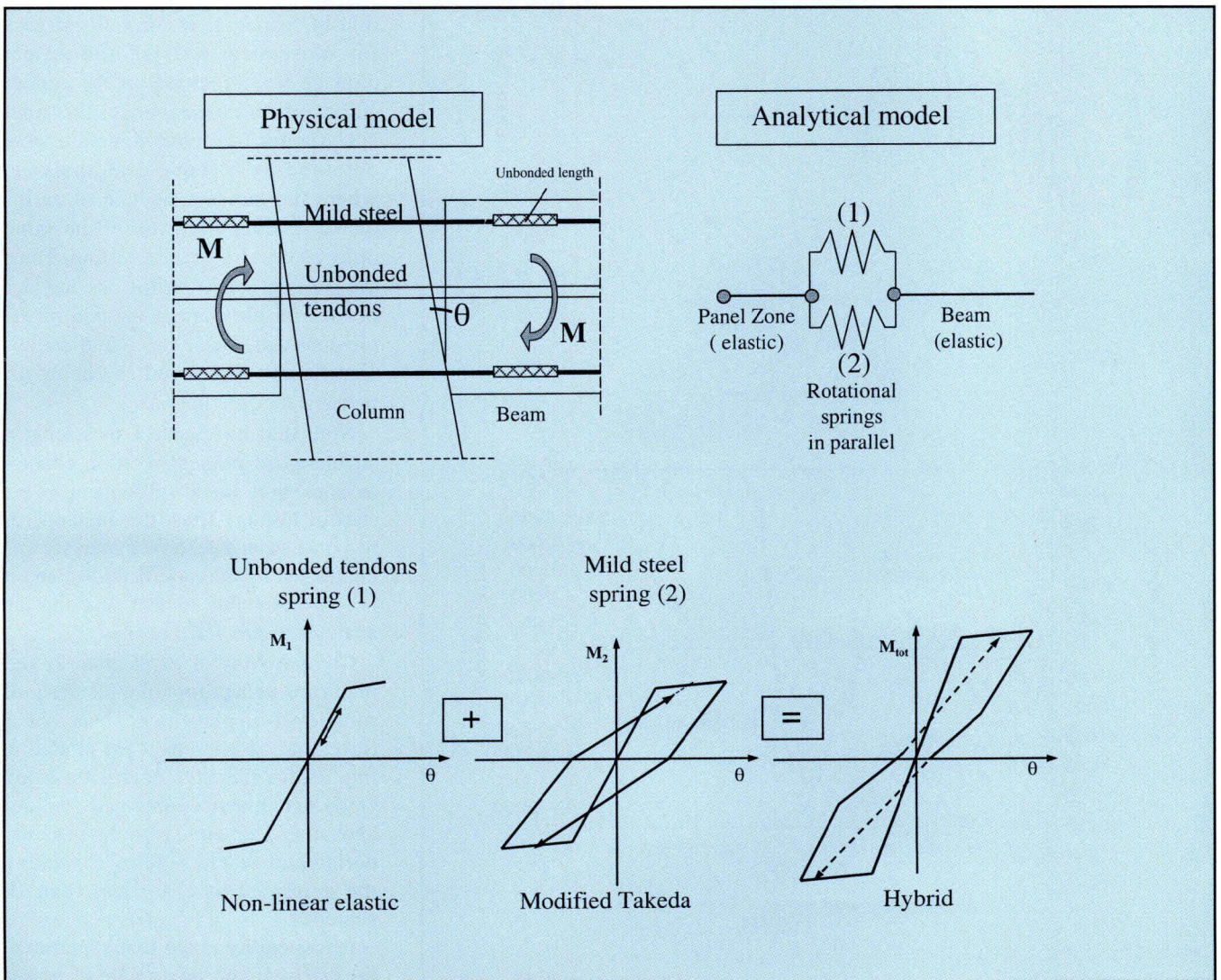


Fig. 28. Analytical model for hybrid prestressed frame connection.

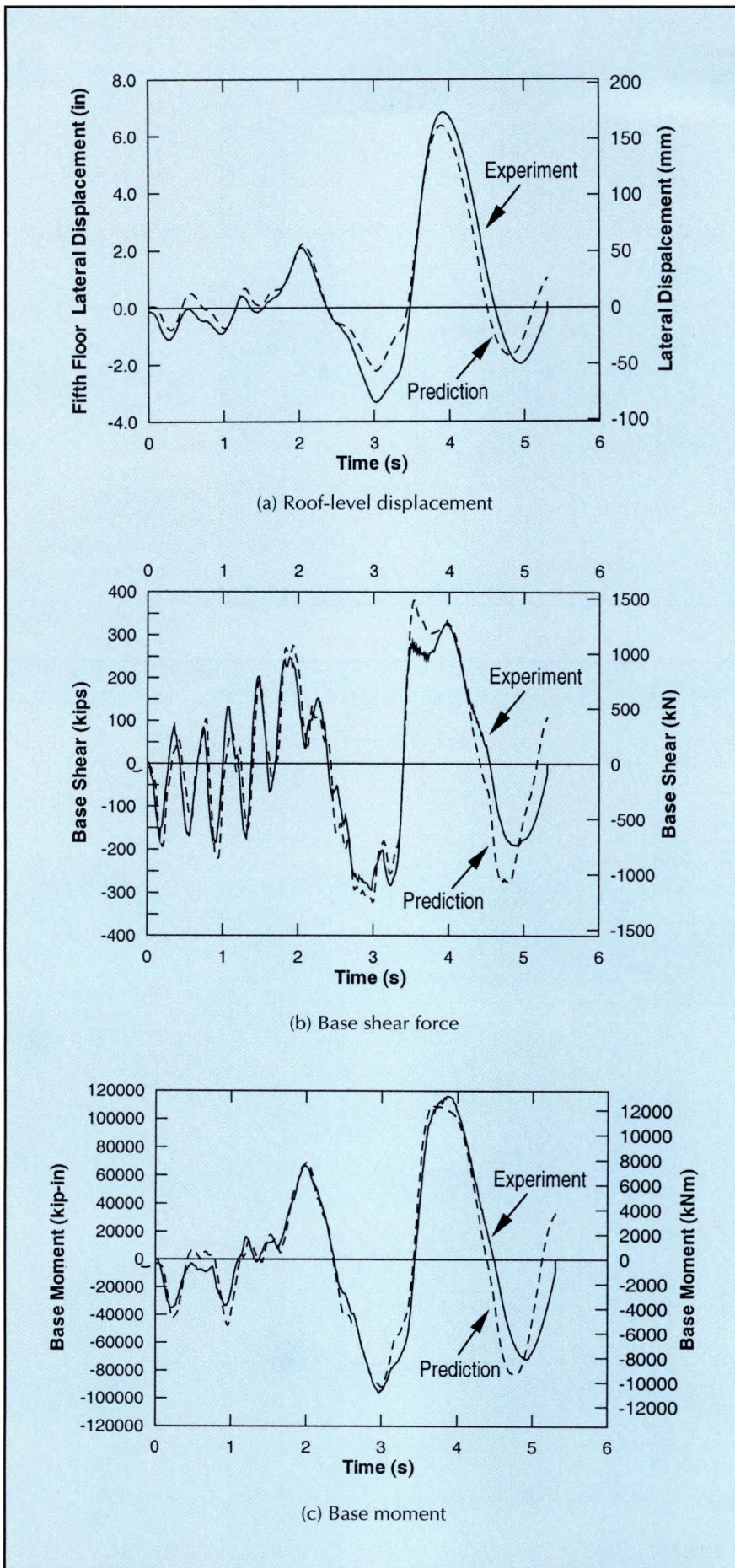


Fig. 29. Comparison of predicted and observed frame response to Zone 4 excitation.

were made subsequent to the tests to improve agreement between the experimental and predicted values.

The first of these involved the hysteretic rule adopted for the energy-dissipating inelastic springs. In the pretest predictions, a bilinear elastoplastic hysteresis rule was used. This was subsequently modified to the Takeda degrading stiffness model, as noted above, which is known to provide better representation of reinforced concrete behavior.

The second modification involved the definition of the initial conditions for the model. In the pretest analyses, each test was predicted independently, as though the frames were initially in the undamaged condition, without having been subjected to the earlier levels of seismic excitation, even though significant inelastic action might have occurred.

With a modified Takeda representation of response, the initial stiffness for subsequent tests should reflect damage and cracking in the earlier stages. As a consequence, the final analyses for the frame direction were obtained by a sequential analysis, where the entire sequence of earthquake records were run in the same order as occurred during testing. Thus, the starting condition for one test depended on the state at the end of the previous test. These two modifications significantly improved (by about 15 percent) the "predictions."

Note that no changes to strength, stiffness, or moment-rotation characteristics were made subsequent to the start of testing. Thus, the envelope of response from a pushover analysis was unaffected by the modifications, and it is felt reasonable to still describe the analyses as predicted results.

Comparisons of experimental and predicted values for time-histories of roof-level displacement, base shear force, and base moment are plotted in Fig. 29 for the EQ2 excitation level. Good agreement is obtained for roof level displacements, with the peak experimental displacements exceeding the predicted level by less than 10 percent.

It was earlier noted that experimental drifts at the design level of response exceeded the design drift by

about the same amount. It is probable that the reason for this increase is the level of damping exhibited by the model.

The moment-displacement hysteresis plots of Figs. 22 and 23 indicate equivalent viscous damping ratios, based on a secant stiffness approximation of about 12 percent with lower values applying for the prestressed frame than for the reinforced frame. This is significantly lower than the design assumption of 20 percent, resulting in increased experimental displacements, despite the increased lateral strength.

Agreement for base shear and moment, as shown in Figs. 29b and 29c is also very satisfactory. The effects of higher mode response in both figures is very similar for both predicted and experimental curves.

A final comparison between the predicted and experimental values is provided by the base moment/roof-displacement envelope response of Fig. 30. In this figure, the results from the analytical pushover analysis are compared with the full set of experimental results, including pseudodynamic tests and inverted triangle tests.

The agreement is satisfactory in the small to moderate displacement range. However, a discrepancy is seen at

large lateral displacements, with the analytical model predicting higher lateral strengths than the experimental values. The reason for this discrepancy is mainly due to not incorporating softening behavior of the beam-column systems, as a result of crushing of concrete and cover spalling in the analytical model.

CONCLUSIONS

The structural response of the PRESSS five-story precast concrete test building under simulated seismic testing was extremely satisfactory. The following summarizes the response and conclusions available at this stage. It is emphasized that additional information will become available as data reduction continues.

1. Damage to the building in the wall direction was minimal, despite being subjected to seismic intensities 50 percent above the design level. Only minor spalling at the wall base, and fine cracking in floor slabs, and near the column bases were observed. The wall was essentially uncracked except at the base during wall direction response. The wall showed additional flexural cracking when subjected to the 4.5 percent out-of-plane drift in the frame direction of re-

sponse. However, these cracks closed up to be invisible to the naked eye at the end of testing.

2. Damage to the building in the frame direction of response was much less than could be expected for an equivalent reinforced concrete structure, subjected to the same drift levels. The performance of the prestressed frame was particularly good, with damage being limited to minor spalling of cover concrete in the beams immediately adjacent to the columns and some crushing of the fiber grout pads at the beam-column interfaces. Crack levels in the beam-to-column joints due to shear were extremely small, and it was evident that the amount of joint shear reinforcement provided, which conformed to current code levels, could have been substantially reduced.

3. Although the non-prestressed frame also performed well, the TCY-gap connections showed more damage, occurring at an earlier stage, than the other connection types. This was due to the inadequate clamping force provided by the bottom post-tensioning, resulting in upwards slip at the beam-column interface under seismic shear forces. Minor changes to the design criteria would correct this problem, but some attention will also be

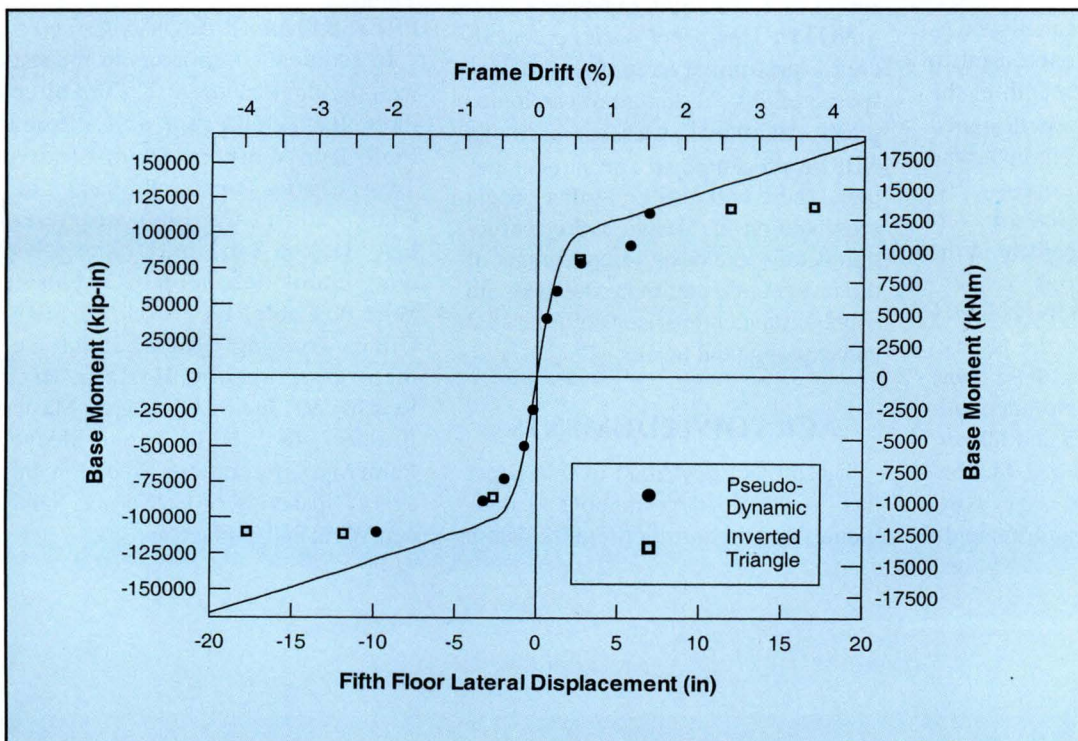


Fig. 30. Comparison of predicted and observed frame direction moment-displacement envelope response.

needed to improve detailing at the beam ends to reduce the tendency for premature spalling of cover concrete.

4. At high levels of response displacements, beam rotation about the longitudinal axis was noted, caused by the high torsional moment induced by the vertical load from the eccentrically supported double-tee floor members, and the reduced torsional resistance in the beam-end plastic hinges. Modified support details should be developed transferring the double-tee reaction closer to the support beam centerline.

5. As anticipated, residual drift after the design level excitation was very low. In the wall direction, the residual drift was 0.06 percent after sustaining a peak drift of 1.8 percent. This corresponds to only 3 percent of the maximum drift. The low residual drift is a characteristic of the unbonded prestressing system used to provide strength in the wall direction,⁵ and is a significant advantage over conventional cast-in-place reinforced concrete construction, where very high residual drifts are possible. The low residual drift was also apparent in the prestressed frame which was based on the same unbonded prestress philosophy. The non-prestressed frame dissipated more energy, but suffered higher residual drifts and somewhat higher damage levels.

6. The test provided an excellent confirmation of the direct displacement-based design approach used to determine the required strength of the building. The structure was designed to achieve drifts of 2 percent under the design level earthquake (Zone 4, UBC intensity), and actually sustained average drifts of 1.8 and 2.2 percent in the wall and frame directions, respectively. This drift is within the accuracy of spectrum-matching for the test accelerograms. The required base-shear strength using direct displacement-based design was only 45 and 60 percent of the strength required by conventional force-based design using UBC provisions for wall and frame di-

rections, respectively.²

7. In the pseudodynamic tests, much higher floor forces were experienced than anticipated. These high force levels were confirmed by analytical studies and were the result of higher mode effects. These high floor force levels represent diaphragm force levels that are significantly higher than currently considered in design and are a consequence of the comparative insensitivity of the higher mode force levels to ductility. Current designs, where force reduction factors are applied equally to higher modes as well as the fundamental mode result in a critical underestimation of the diaphragm force levels. The influence of higher mode floor forces is also translated into story shear force levels, and moment distributions that are more severe than currently considered in American designs using an inverted triangular distribution of the base shear force. However, the distributions of peak story shear force and overturning moment were well predicted by established procedures.⁶

8. Simple analytical models, suitable for the design office, were used to predict the response of the building. These were found to provide very good simulation of response, with excellent correlation between predicted and observed displacements, story shears, and overturning moments.

NOTE: This paper must be considered a preliminary report on the response of this substantial research program. Additional experimental results will be presented in subsequent papers. There will also be further papers presented on the design and construction details, the design implications of the test results, and more detailed and sophisticated comparisons of predicted and experimental results.

ACKNOWLEDGMENTS

The project described in this paper has involved a large number of individuals and organizations, all of whom

deserve individual thanks and acknowledgment. A full list would be impossibly long. Of particular importance are Dr. Chris Latham (UCSD) and Professor Akira Igarashi (Kyoto University) whose efforts in solving the extremely difficult problems of controlling the pseudodynamic tests were essential to the test success.

The efforts of the building designers, Professor John Stanton (plus University of Washington graduate students), and Ms. Suzanne Nakaki, who not only did a superb job of the building design, as evidenced by its excellent performance, but also were present during most of the long-night testing sessions, are particularly acknowledged.

Primary financial support for the PRESSS research program was provided by the PCI (Precast/Prestressed Concrete Institute), the NSF (National Science Foundation), and the PCMAC (Precast/Prestressed Concrete Manufacturers Association of California). The extent of industry support, in terms of financial assistance, material donation, technical advice, and provision of precast products is unparalleled in major United States structural research projects.

Special thanks are due to Mario J. Bertolini, chairman of ATLSS and PRESSS Ad Hoc Committee, and Thomas J. D'Arcy, chairman of the PRESSS Phase III Advisory Group.

In addition, contributors to the testing program include A. T. Curd Structures, Inc.; BauTech, Co.; California Field Iron Workers Administrative Trust; Charles Pankow Builders, Ltd.; Clark Pacific; Coreslab Structures, L.A.; Dayton Superior; Dywidag Systems International; ERICO; Florida Wire & Cable, Inc.; Fontana Steel; Gillies Trucking; Heated Reinforcement Corporation; Horizon High Reach; JVI, Inc.; LG Design; Master Builders, Inc.; NMB Splice Sleeve; Pomeroy Corporation; Precision Imagery; Spancrete of California; Sumiden Wire; and White Cap.

REFERENCES

1. Priestley, M. J. N., "The PRESSS Program — Current Status and Proposed Plans for Phase III," *PCI JOURNAL*, V. 41, No. 2, March-April 1996, pp. 22-40.
2. Nakaki, S. D., Stanton, J. F., and Sritharan, S., "An Overview of the PRESSS Five-Story Precast Test Building," *PCI JOURNAL*, V. 44, No. 2, March-April 1999, pp. 26-39.
3. Priestley, M. J. N., "Displacement-Based Approaches to Rational Limit States Design of New Structures," Keynote Address, 11th European Conference on Earthquake Engineering, Paris, September 1998.
4. Priestley, M. J. N., and Kowalsky, M. J., "Direct Displacement-Based Design of Buildings," *Bulletin of the NZ National Society for Earthquake Engineering*, 1999.
5. Priestley, M. J. N., and Tao, J. T., "Seismic Response of Precast Prestressed Concrete Frames with Partially Debonded Tendons," *PCI JOURNAL*, V. 38, No. 1, January-February 1993, pp. 58-69.
6. SEAOC Performance Based Seismic Design Ad Hoc Committee, "Tentative Performance Based Seismic Engineering Guidelines - SEAOC Blue Book, Appendix G," 1998.
7. Sritharan, S., Igarashi, A., Priestley, M. J. N., and Seible, F., "Test Design of the PRESSS Five-Story Precast Concrete Building," Proceedings, 68th Annual Convention, Structural Engineers Association of California, Santa Barbara, CA, 1999, pp. 255-261.
8. Conley, J., Priestley, M.J.N., and Sritharan, S., "Wall Direction Modeling of the Five-Story PRESSS Precast Test Building," Report SSRP 99/19, University of California, San Diego, CA, 1999.
9. Pampanin, S., Priestley, M. J. N., and Sritharan, S., "Frame Direction Modeling of the Five-Story PRESSS Precast Test Building," Report SSRP 99/20, University of California, San Diego, CA, 1999.
10. Igarashi, A., Seible, F., Hegemier, G., and Priestley, M. J. N., "The U.S.-TCCMAR Full-Scale Five-Story Masonry Research Building Test, Part III - Seismic Load Simulation," Report SSRP-94/03, University of California, San Diego, CA.
11. Paulay, T., and Priestley, M. J. N., *Seismic Design of Reinforced Concrete and Masonry Buildings*, John Wiley and Sons, New York, NY, 1992, 786 pp.
12. Carr, A. J., "Ruaumoko Program for Inelastic Dynamic Analysis — Users Manual," Department of Civil Engineering, University of Canterbury, Christchurch, New Zealand, 1998.
13. Takeda, T., Sozen, M., and Nielsen, N., "Reinforced Concrete Response to Simulated Earthquakes," *Journal Structures Division*, ASCE, V. 96, No. 12, December 1970.